Title
A STUDY OF THE KINETICS OF THE REACTION H + 02 BY PARAMAGNETIC RESONANCE.

Author
Edelstein, Norman Marvin.

Publication Date
1962-04-01

UCRL 10108

University of California

Ernest O. Lawrence Radiation Laboratory

A STUDY OF THE KINETICS OF THE REACTION $H + O_2$ BY PARAMAGNETIC RESONANCE

Berkeley, California

DISCLAIMER

Research and Development

UCRL-10108
UC-4 Chemistry
TID-4500 (17th Ed.)

UNIVERSITY OF CALIFORNIA

Lawrence Radiation Laboratory

Berkeley, California

A STUDY OF THE KINETICS OF THE REACTION H + O_2 BY PARAMAGNETIC RESONANCE

Norman Marvin Edelstein

(Ph.D. Thesis)

April 1962

Printed in USA. Price $1.75. Available from the
Office of Technical Services
U. S. Department of Commerce
Washington 25, D.C.

THE STUDY OF THE KINETICS OF THE REACTION H + O_2 BY PARAMAGNETIC RESONANCE

Contents

ABSTRACT

The gas-phase reaction of H atoms with O_2 has been studied as a function of the total pressure and of the partial pressure of O_2. An electron spin resonance spectrometer was used to analyze for the relative steady-state concentration of the H atoms in a flow system.

In order to determine the effect of heterogeneous recombination of H atoms on the walls of the quartz reaction tube, the disappearance of H atoms in an H atom - H_2 system and in an H atom - H_2-argon system was also studied. The experimental results were explained by a modified diffusion equation. The recombination coefficient γ for H atoms was determined and the value found was $1.8 \pm .7 \times 10^{-5}$.

The experiments on the H atom - O_2 reaction showed that the rate of decay of the H atoms was inversely proportional to the total pressure. The rate constants for this reaction were calculated from the experimental data by the addition of an extra term to the modified diffusion equation. The following mechanism has been proposed to explain the experimental results:

$$H + O_2 \xrightarrow{k_a} HO_2^*,$$

$$HO_2^* \xrightarrow{k_b} H + O_2,$$

$$HO_2^* + \text{Wall} \xrightarrow{k_w} HO_2 + \text{Wall},$$

$$H + HO_2 \xrightarrow{k_d} 2OH,$$

$$H + OH + M \xrightarrow{k_f} HOH + M.$$

On the assumption of steady-state conditions for HO_2^*, OH, and HO_2, this mechanism gives, for the disappearance of H atoms,

$$-d(H)/dt = 4k_a k_w (H)(O_2)/k_b .$$

At the pressures used k_w is inversely proportional to the total pressure, and the lifetime of HO_2 ($1/k_b$) was calculated to be $5 \pm 2 \times 10^{-10}$ sec.

I. INTRODUCTION

The microwave absorption spectrum of the OH radical, discovered by Townes et al. in 1953,[1] gives one a direct way of studying this unstable species. This method has high sensitivity and is relatively convenient, but it is limited, because of pressure broadening of the absorption lines, to systems of a total pressure not greater than 1 mm Hg. Investigations of the kinetics of the formation of OH by the reaction of H atoms and O_2 were made in this laboratory by use of the microwave spectrometer as an analytical tool.[2,3] Interpretation of the data proved difficult because of the profusion of conflicting results concerning the early steps of the reaction mechanism, and so this investigation was undertaken to elucidate the initial steps of the H plus O_2 reaction. In order to follow this reaction we chose to study the decay of the H atoms in O_2 by means of their electron spin resonance absorption.

Berginer and Heald studied the electron spin resonance spectrum of H atoms in 1954.[4] Since then various workers have used electron spin resonance to analyze for H atoms. Shaw studied the dissociation of H_2 in a microwave discharge[5] and also the effect of water vapour on the extent of the dissociation of the H_2.[6] Hildebrandt et al. have developed methods for the quantitative measurement of H atoms.[7,8] Since OH[9], O_2,[10] and in principle HO_2 (an intermediate species in the reaction) have electron spin resonance spectra, we could in theory study four reacting species in the reaction $H + O_2$. We did in fact see spectra due to OH and O_2, but this line of research was not continued. All our significant work was done by following the decay of H atoms upon reaction with O_2 by means

of electron spin resonance.

H atoms were generated by means of a microwave discharge in H_2, the O_2 was added to the mixture of H atoms and H_2, and the reacting mixture was pumped down a long cylindrical tube which ran through the resonant cavity of the electron spin resonance spectrometer. The cylindrical tube and the associated gas system were portable, so that measurements of the H atom concentration could be made along the tube by moving the apparatus back and forth with respect to the spin resonance cavity. In order to be sure that we were studying the correct reaction, the decay of H atoms without O_2 was also studied by this technique. A more detailed discussion of the experiments is presented later. First a summary of the relevant previous work on the H atom - O_2 reaction, and on the recombination of H atoms, is given.

A. Meyer's Work

By use of a glass-cell microwave spectrometer, R. T. Meyer conducted some studies on the low-pressure reaction ($P_{total} < 1$ mm Hg.) of H atoms and O_2.[3] He observed the OH absorption line as a function of both the oxygen partial pressure and the total gas pressure. In these experiments Meyer mixed H atoms (in H_2) with O_2. The gases were mixed in a short section of 12-mm o.d. quartz tubing and then led into a length of 45-mm o.d. ordinary pyrex tubing. The low time in the 15-mm tubing was less than 0.01 sec, and in the 45-mm tubing about 1 sec. The larger tubing was equipped with a 4-mm quartz rod mounted along its axis for propagation of microwaves. In these experiments Meyer measured the OH radical absorption in the vicinity of the rod. He found that the OH concentration was fairly uniform down the length of the rod. He also

found that initially the OH concentration increases with O_2 concentration but subsequently it levels off. His measurements also showed that the OH concentration is roughly inversely proportional to total pressure at constant O_2 pressure, and that the surface condition of his cell did not significantly affect the concentration of OH radicals.

The mechanism which Meyer proposed to explain his measurements is as follows:

$$H + O_2 \rightarrow HO_{2}^{*}, \qquad k_a = 3.2 \text{ z } 10^{11} \text{ l/mole sec}; \qquad \text{(a)}$$

$$HO_{2}^{*} \rightarrow H + O_2, \qquad k_b = 1 \times 10^{11} \text{ sec}^{-1}; \qquad \text{(b)}$$

$$HO_{2}^{*} \rightarrow HO_2 + h\nu, \qquad k_c = 1 \times 10^{6} \text{ sec}^{-1}; \qquad \text{(c)}$$

$$H + HO_2 \rightarrow 2OH, \qquad k_d = 7.3 \times 10^{11} \text{ l/mole sec}; \qquad \text{(d)}$$

$$OH + HO_2 \rightarrow H_2O + O_2, \qquad k_e = 3 \times 10^{11} \text{ l/mole sec}; \qquad \text{(e)}$$

$$H + OH + M \rightarrow HOH + M, \qquad k_f = 4.9 \times 10^{11} \text{ l}^2\text{/mole}^2 \text{ sec}. \qquad \text{(f)}$$

Assuming steady-state conditions of HO_{2}^{*}, HO_2, and OH, this mechanism gave an OH concentration under some conditions which was directly proportional to the square root of O_2, and inversely proportional to the square root of the total pressure. This mechanism qualitatively fitted his data.

Using the values for the rate constants given above, Meyer obtained a reasonable value for the steady-state concentration of OH. The rate constants k_a, k_b, k_e, and k_f were obtained from other data and are discussed in the next part. The stabilization of HO_{2}^{*} by emission was chosen in order to give the observed total pressure dependence of the OH radical. The value of k_c was chosen slightly greater than the rate of collisional deactivation at a total pressure of 1.0 mm Hg. The value of k_e was estimated from the kinetic theory of gases.

B. Other Work on the Reaction $H + O_2$

The literature on this reaction is quite voluminous. We shall discuss briefly only the results that are pertinent to the problem of low-pressure room-temperature reaction. A fairly complete review is given by Meyer.[3]

First, the reaction $H + O_2 \rightarrow OH + O$ is 15.5 kcal endothermic.[2] Therefore we can eliminate this reaction, since it is too slow at room temperature to be of importance.

Secondly, the important gas-phase product of the reaction is HOH; experimental evidence seems to indicate that H_2O_2 is not an important stable product.[3] Foner and Hudson's work[11] is strong evidence for the existence of the HO_2 radical. Their experiments are based on the use of the mass spectrometer. Although they detected HO_2^+ only at higher pressures, Robertson, who also did mass spectroscopic work, saw HO_2^+ in the low pressure reaction.[12] He found that the HO_2^+ increased with pressure and suggested the mechanism

$$H + O_2 \rightarrow HO_2^*,$$
$$HO_2^* \rightarrow H + O_2,$$
$$HO_2^* + M \rightarrow HO_2 + M,$$

and estimated the lifetime $1/k_b$ of HO_2^* as 5×10^{-12} sec. Burgess and Robb studied the rate of the mercury-photosensitized hydrogen-oxygen reaction by measuring the heat liberated in the system.[13] The pressure range they covered was from 5 to 150 mm Hg. The rate constants k_a and k_d in the previous section are taken from their data. In the range of pressures for their experiments, collisional deactivation of HO_2^* was

the important mechanism. They estimated the lifetime of HO_2^* as 4.0×10^{-9} sec. The value of k_f in the previous section was taken from the spectroscopic work of Oldenberg and Riecke on the disappearance of OH radicals.[14]

The literature contains many contradictory results from many types of indirect measurements. This is why the direct observation of one of the primary reacting species seemed such a promising line of research.

C. Recombination of Atoms

While we were primarily interested in studying the gas-phase reaction of $H + O_2$, we found that heterogeneous reactions were important in our low-pressure system. In particular, we found that the heterogenous recombination of H atoms could be followed, and one of the results of this thesis is new data on this reaction.

Studies on the disappearance of H atoms have been conducted by many investigators.[15-19] At low pressures ($\approx$ 0.5 mm Hg) and high surface-to-volume ratios, the heterogeneous reaction of H atoms on the walls of the vessel is the important reaction taking place. Experimental data show that the reaction is first order with respect to H atoms. The mechanism suggested to explain the data says that first a layer of H atoms is adsorbed on the surface of the vessel.[20] The surface becomes fully covered--that is, saturated with H atoms. Then H atoms in the gas phase diffuse to the saturated surface and react. The important experimental parameter measured is γ, the recombination coefficient. This constant, γ, is defined as the ratio of the number of atoms striking and reacting with the surface to the total number of atoms hitting the surface. Values of γ have been measured for water-poisoned pyrex and quartz

surfaces and have ranged between 10^{-4} and 10^{-6}.[15,17,18]

Recently Wise and Ablow have mathematically analyzed the diffusion and heterogeneous reaction of H atoms in a cylinder.[19] In a later paper they include in their treatment the effects of convective flow and second-order gas-phase recombination of H atoms.[21] A mathematical treatment similar to Wise and Ablow's is used in this thesis. The model and mathematical analysis are later discussed in detail.

Krongelb and Strandberg, in their study on O atoms, were the first to apply the techniques of electron spin resonance to the study of heterogeneous and homogeneous reactions of atoms.[22] They employed two methods. One is to allow O atoms to diffuse into a sidearm of the main reaction vessel and measure the steady-state concentration of O atoms at different places along the sidearm. This was done by moving it back and forth in the detection cavity. The other method used was a flow method. The oxygen atoms flowed directly through the detection cavity. The discharge cavity was moved back and forth along the tube in order to change the flow distance. They measured γ for the O atom heterogeneous surface reaction, and also obtained a rate constant for the homogeneous recombination of O atoms in the gas phase. The mechanism proposed to explain their data is similar to the one mentioned previously for H atoms.

In summary we can say that the disappearance of H atoms by heterogeneous reaction is a process of first order in H atoms. The mechanism that explains the results of a wide number of experiments is the diffusion of a gas-phase H atom to the surface of the vessel, where it reacts with an H atom adsorbed on the surface.

II. EXPERIMENTAL METHOD

A. Spectrometer

An X-band spectrometer operating near 9,000 Mc/sec, which was constructed in this Laboratory, was used for the measurements reported in this thesis. It is a conventional balanced-bridge type of spectrometer employing 100-cycle magnetic field modulation. A block diagram of the instrument is shown in Fig. 1. A Varian electromagnet with 6-in. diameter pole pieces with ring shims together with a stabilized power supply provided the d.c. magnetic field.

A Laboratory for Electronics stabilized klystron was employed as a frequency source. The klystron is stabilized on a discriminator cavity which provides an error signal to the reflector. Changing the bias on the crystals in the discriminator cavity permitted a fine tuning of the klystron frequency. This proved a very convenient method for manually adjusting the frequency of the klystron on the sample cavity.

Flat-wound coils mounted over the pole pieces provided the 100-cycle field modulation. These coils were fed from the Zeeman modulator unit which also provided a reference signal for the phase-sensitive detector. The current in the coils could be accurately adjusted and the magnitude was monitored by a Hewlett-Packard a.c. voltmeter and a Hewlett-Packard current probe. A tuned 100-cycle preamplifier of conventional low-noise design was mounted near the detector crystal. The signal was amplified by the main tuned amplifier, and then fed into the phase-sensitive detector, whose output could be traced out on a recording potentiometer.

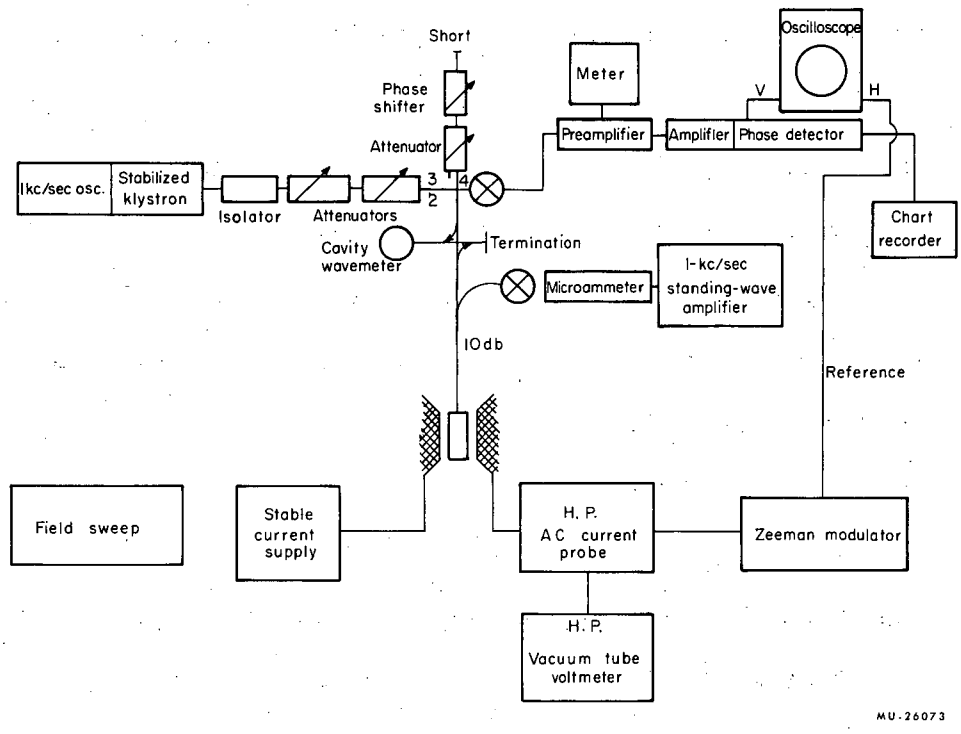

Fig. 1. Block diagram of the X-band spectrometer.

The cavity used for these measurements operated in the TE_{011} mode. It was made from a cylindrical piece of quartz which fitted into two silver-plated brass end plates. The inside of the cavity was coated with a Du Pont silver emulsion which was air-dried and then baked onto the quartz. In order to get the best Q, the cavity was polished with commercial silver polish. The cavity was coupled through one of the end plates in the style developed by Strandberg et al.[22]

B. Gas System

In order to perform the necessary experiments a portable vacuum system was built. This consisted of mounting the necessary flowmeters, pressure gauges, and discharge equipment on a cart which could roll on narrow-gauge railroad tracks.[23] This arrangement allowed the tube containing the reacting mixture to be easily moved with respect to the cavity and the magnet. A block diagram of the flow is shown in Fig. 2. The oxygen (Matheson technical grade, 99.6% min assay as O_2) and argon (Matheson technical grade, 99.9% min assay as Ar) used in these experiments came straight from their respective cylinders and were used without purification. Hydrogen (Matheson prepurified, 99.9% min assay as H_2) at 1 atmosphere pressure flowed through an activated charcoal trap at room temperature and then was bubbled through water. The water was added to increase the percentage dissociation of hydrogen molecules. All flow rates were monitored at 1 atmosphere pressure either with calibrated dibutyl phthalate manometers or Fischer and Porter calibrated flowmeters. Flow rates were controlled by use of Hoke needle valves. Total pressure in the reaction tube was measured by a McLeod gauge.

A diagram of the quartz reaction tube is shown in Fig. 3. It

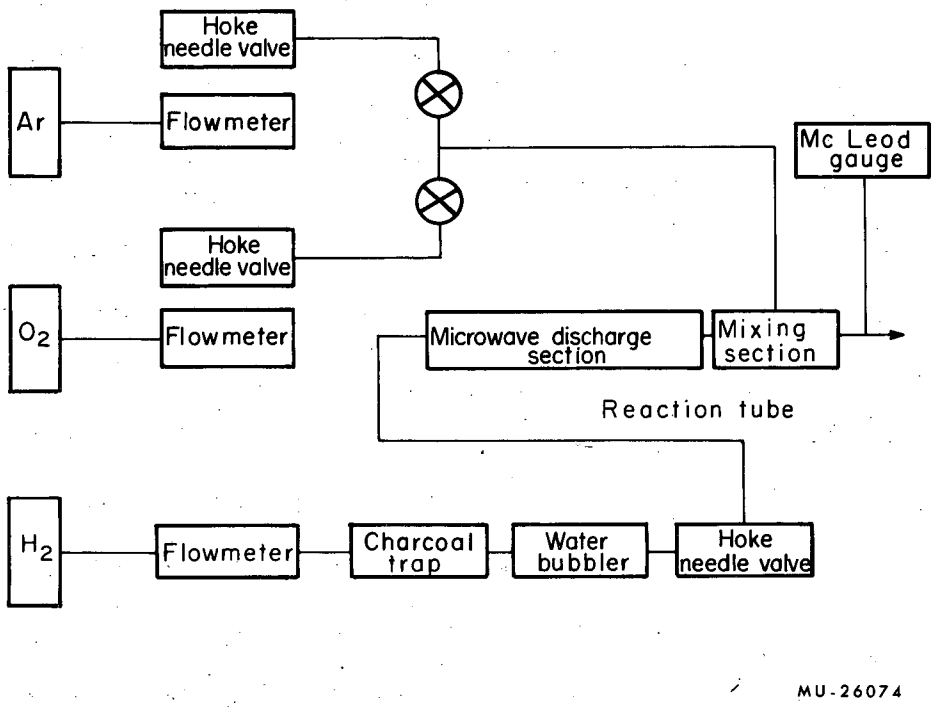

Fig. 2. Block diagram of flow system.

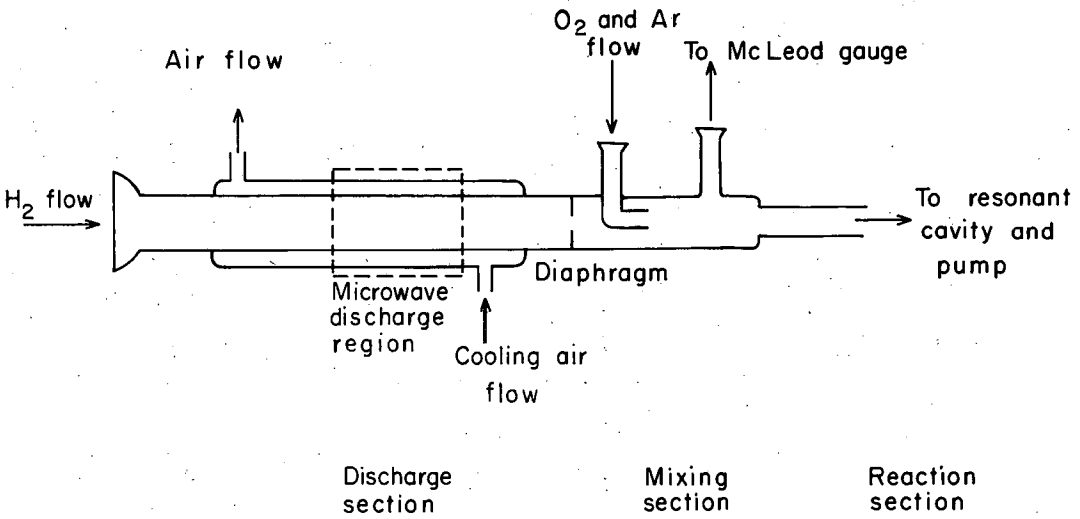

Fig. 3. Quartz reaction tube.

consists of three sections, the discharge section, the mixing section, and the reaction section. The discharge section consisted of two concentric tubes, the inner tube being part of the vacuum system and separated from the mixing section by a diaphragm with a 1-mm-diam hole in the center. The outer quartz tube is a jacket which fits over the inner discharge tube and is used to cool the discharge region and its resulting gas. In this way the walls of the discharge section closest to the mixing section are kept at room temperature.

Hydrogen molecules and atoms flowed through the diaphragm into the mixing section. At this position another tube concentric with the larger tube added O_2 and sometimes a third body into the flow system. Then the gaseous mixture flowed down the reaction section, which was approximately 120 cm long. Two quartz tubes of different diameters were used for the reaction section. The larger had an i.d. $0.92 \pm .03$ cm and the smaller had an i.d. $0.72 \pm .03$ cm. The total pressure was measured at a point between the mixing section and the reaction section. The reaction tube was connected to the rest of the vacuum system by means of two long tubes connected to each other and to the rest of the system by ground glass ball joints whose axes were perpendicular to the magnet pole face. This arrangement allowed the reaction tube, which passed through the spectrometer cavity located between the pole faces of the magnet, to be moved back and forth, without breaking the vacuum and without using flexible tubing, in the plane parallel to the pole faces in the center of the magnet gap. A Welch #1379B vacuum pump, which has a pumping speed of 370 liters/min at 1 mm Hg, was used.

A CW 50-watt QK60 magnetron was used to produce the discharge.

The 10-cm microwave power was fed into a TM_{010} cavity with the quartz discharge tube in the center. During some of the early experiments a Wrede gauge was used to measure the percentage dissociation of hydrogen.[24] A Decker Corporation differential pressure meter #306 was used to measure the difference in pressure across the effusion hole.

C. Measurements of Hydrogen Atom Concentration

The hydrogen atom concentration was measured by sweeping through the high-field H atom line[4] a number of times. Then the average value of the peak height of the first derivative of the absorption curve was obtained and used as a measure of the concentration of H atoms in the cavity. This approximation is valid only if the line width does not change with the concentration of H atoms or with total pressure.[7,8] The line width in these experiments is determined by modulation broadening and by the inhomogeneity of the magnetic field, and is approximately 2.5 gauss. The line-width broadening effects of electron exchange[25] and the total pressure are on the order of 0.3 gauss,[7] and are relatively small compared with the experimental line width. Therefore the H atom concentration was assumed to be proportional to the peak-to-peak height.

In order to compensate for the change in Q of the cavity when the reaction tube was moved, and for the change of the sensitivity of the spectrometer with time, a sample of DPPH (1,1-diphenyl -2-picryl hydrazyl) was placed in the cavity. The following procedure was used. First the H atom line was swept through a number of times (at least three) and then the DPPH resonance line was swept through a number of times. The amplitude of the 100-cycle magnetic field modulation was set to give the maximum H atom signal. When the DPPH

line was swept through, the modulation amplitude was set so as to give a signal about half as large as the initial H atom signal. The amplitudes of the modulation for both the H atom line and the DPPH were chosen at the start of a run and were kept constant throughout the run. A run consisted of a series of measurements along the tube, each measurement being at least 10 cm further down the tube than the previous one. The flows of gases and the total pressure were kept constant during a run. Measurements with the Wrede gauge showed that the percentage dissociation of hydrogen remained constant throughout a run. All H atom concentrations are presented as the ratio of the H atom signal to the DPPH signal. This method was particularly useful and simple in these experiments, since the DPPH line is about 200 gauss away from either H atom line.

D. Experimental Results

Two types of measurements were made. One was the disappearance of H atoms without any oxygen present, and the other was the change in this reaction when oxygen was added to the system. These two types of experiments are discussed individually and then the results are correlated in the next section.

1. H in H_2

At the start of our work the reaction tube was cleaned with nitric acid, rinsed with distilled water, and the coated with 1 M solution of orthophosphoric acid. Later, Dri-Film (dimethyl-dichloro-silane) was tried as a coating, and also a straight chain paraffin, dotriacontane ($CH_3(CH_2)_{30}CH_3$). Another procedure was also tried and finally used in most of the runs. In this method, the tubes were cleaned with dilute

hydrofluoric acid and then rinsed with distilled water. This process left cleaned quartz as the surface. A change in the surface appeared to have little effect on the rate of recombination of the H atoms except in the case of dotriacontane. No H atom resonance was seen with this paraffin coating. It was also observed that this coating was slowly removed by the H atoms. It should also be mentioned that with any of the coatings applied to the surface (as well as with cleaned quartz) there was a period of aging of the tube (usually a few hours of flow) before reproducible measurements could be made.

In some experiments the water in the hydrogen bubbler was held at $0^{\circ}C$. This was done in order to reduce the amount of water vapor in the reaction tube by a factor of four and to see the effect on the rate of recombination of the H atoms. There was no noticeable change of the rate. Therefore one concludes that once the water vapor has reached a certain concentration, an increase of this concentration does not affect the rate of recombination as long as the total amount of water present is small compared with the reactants.

The hydrogen atom recombination data were plotted as the logarithm of the intensity of the H atom signal (in arbitrary units) vs the distance from the mixing section of the tube (in cm). The decrease in intensity (or concentration) with distance followed a first-order rate law and formed straight lines on these plots. This agrees with previous work.[20] The important quantity obtained from the plots was the distance required for half of the reaction to take place.

Plots of the experimental points are shown in Figs. 4 through 12. The experimental error, which was due to uncertainties in the intensity measurements, is estimated to be about 10 to 25%, the error increasing

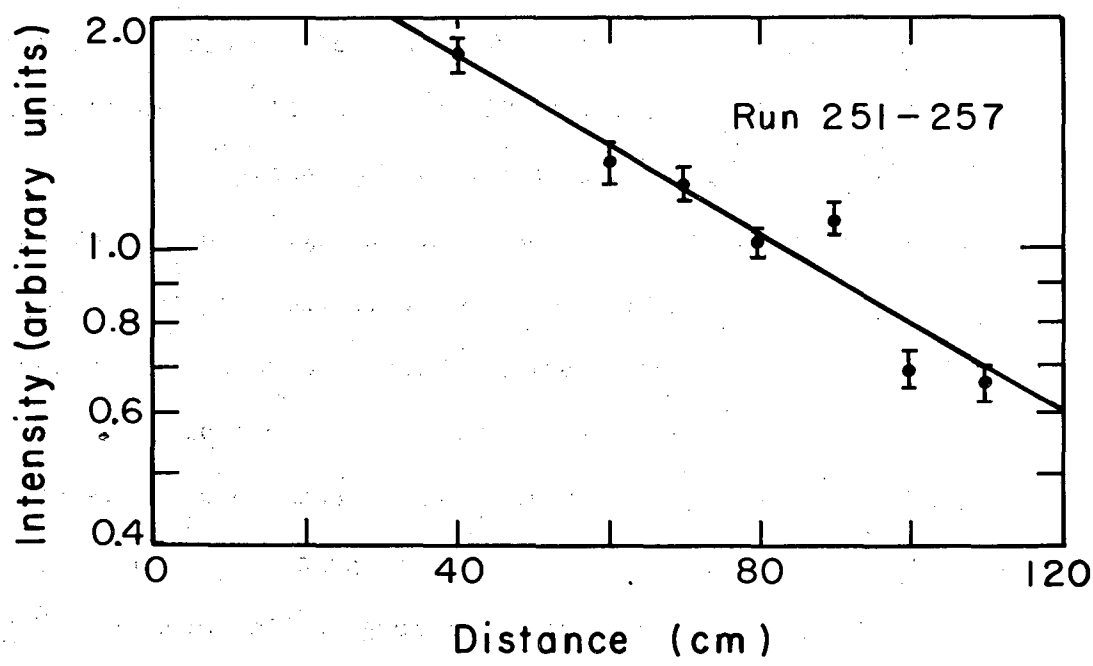

Fig. 4. H atom–H_2 system. Flow H_2, 4.0 cc/min; total pressure, 24 mm Hg; surface, H_3PO_4.

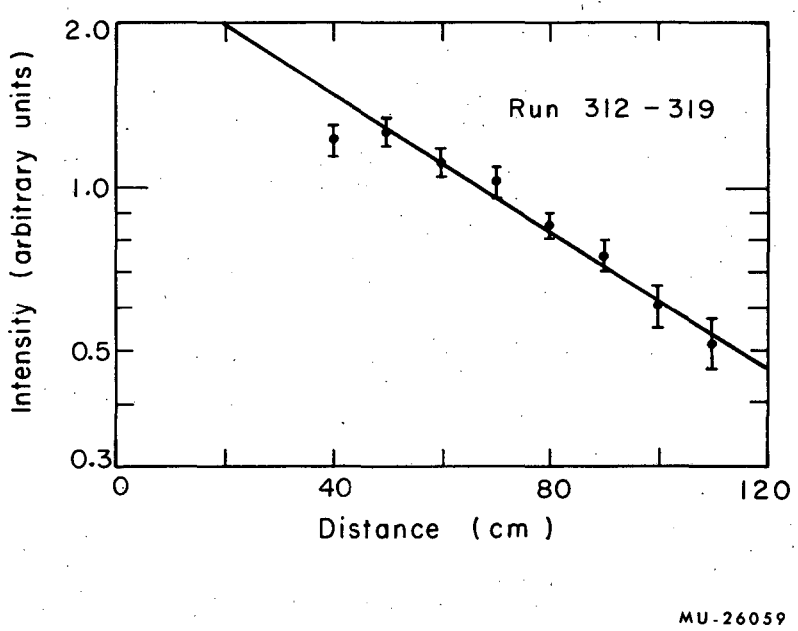

Fig. 5. H atom–H_2 system. Flow H_2, 4.2 cc/min; total pressure, 0.25 mm Hg; surface, quartz.

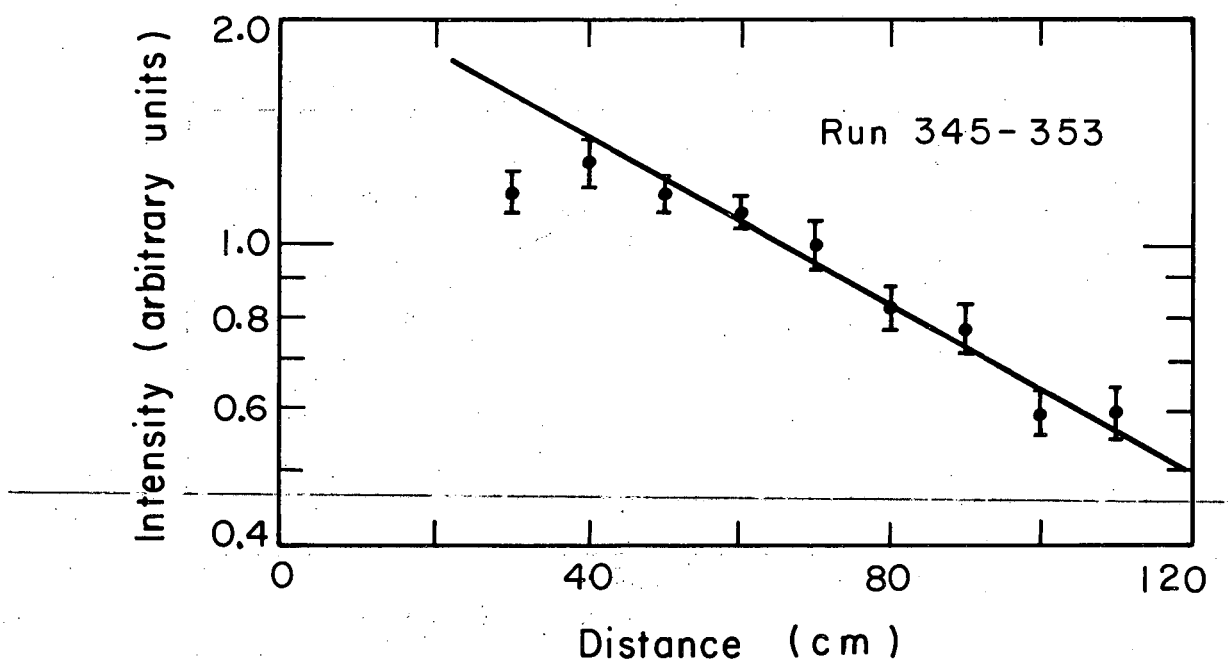

Fig. 6. H atom–H_2 system. Flow H_2, 5.8 cc/min; total pressure, 0.33 mm Hg; surface, quartz.

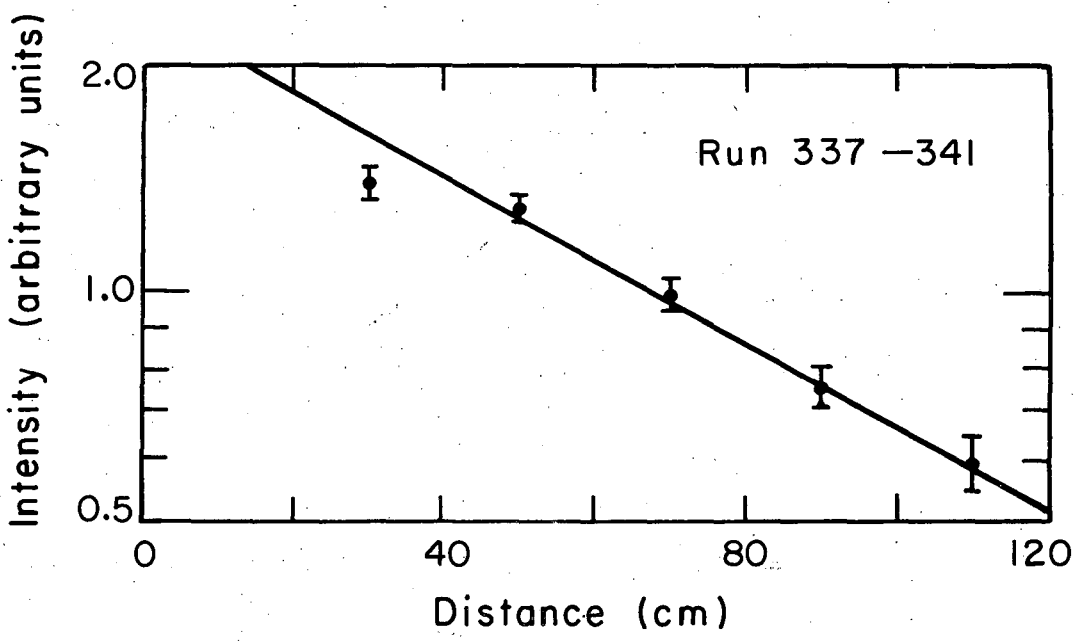

Fig. 7. H atom–H_2 system. Flow H_2, 6.3 cc/mm; total pressure, 0.37 mm Hg; surface, Dri-Film.

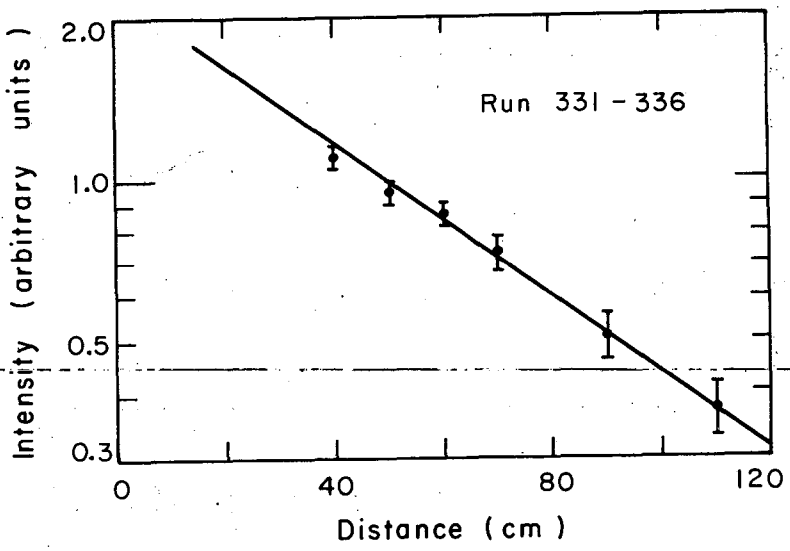

Fig. 8. H atom–H_2 system. Flow H_2, 6.5 cc/min; total pressure, 0.38 mm Hg; surface, Dri-Film.

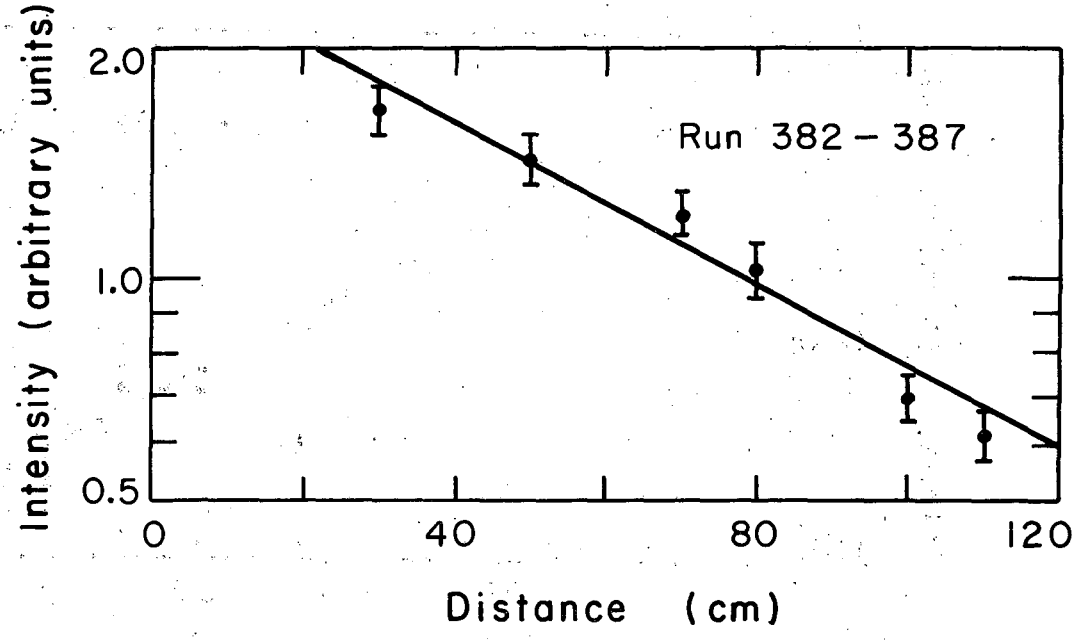

Fig. 9. H atom–H_2 – A system. Flow H_2, 1.5 cc/min; Flow A, 4.8 cc/min; total pressure, 0.43 mm Hg; surface, quartz.

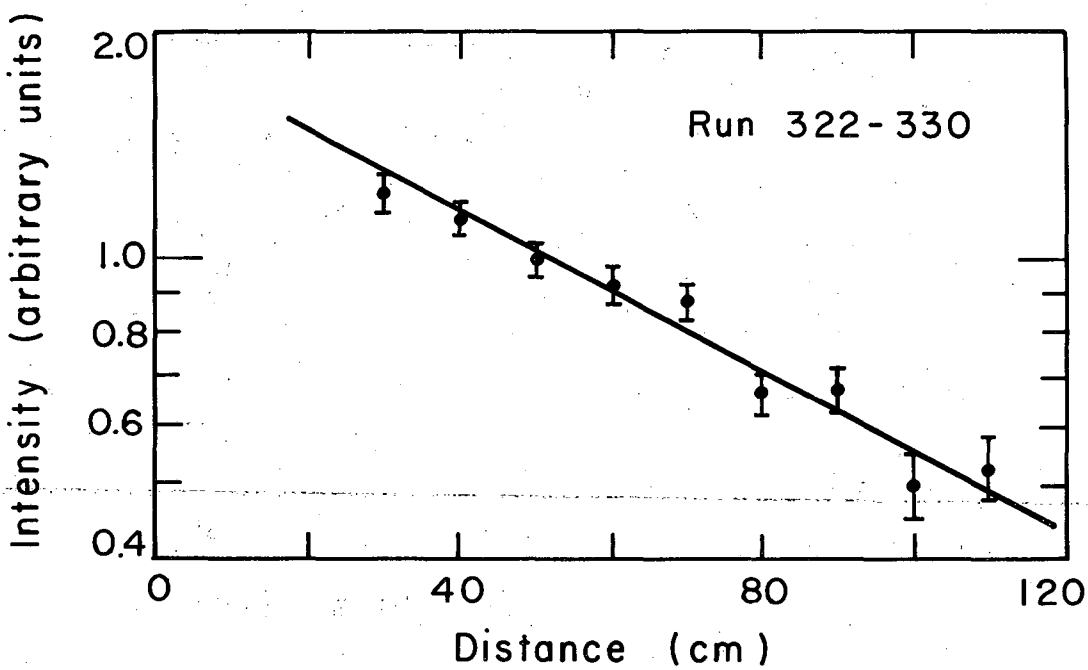

Fig. 10. H atom–H_2 system. Flow H_2, 8.1 cc/min, total pressure, .45 mm Hg; surface, quartz.

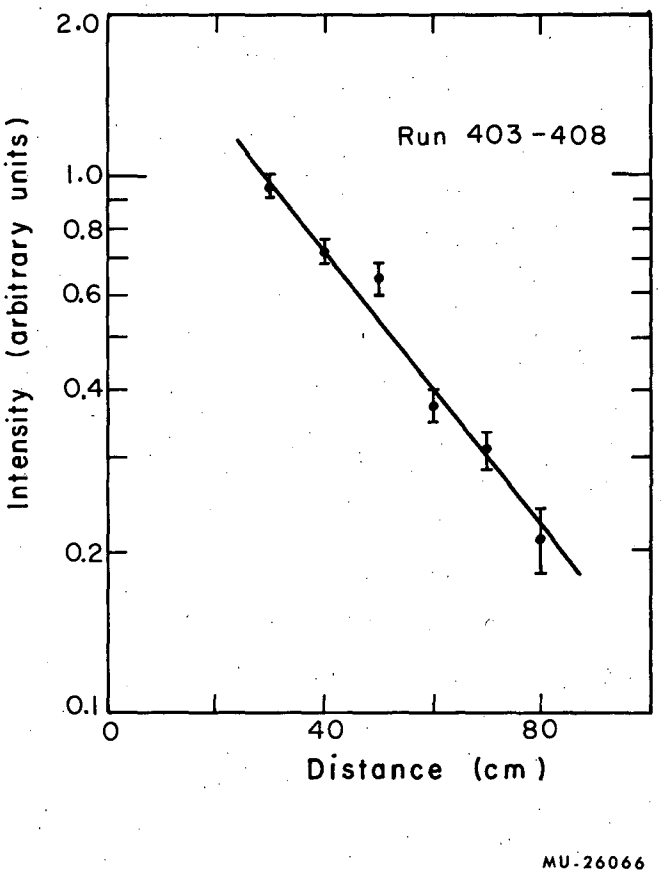

Fig. 11. H atom–H_2 system. Flow H_2, 0.9 cc/min; total pressure, 0.91 mm Hg; surface, quartz.

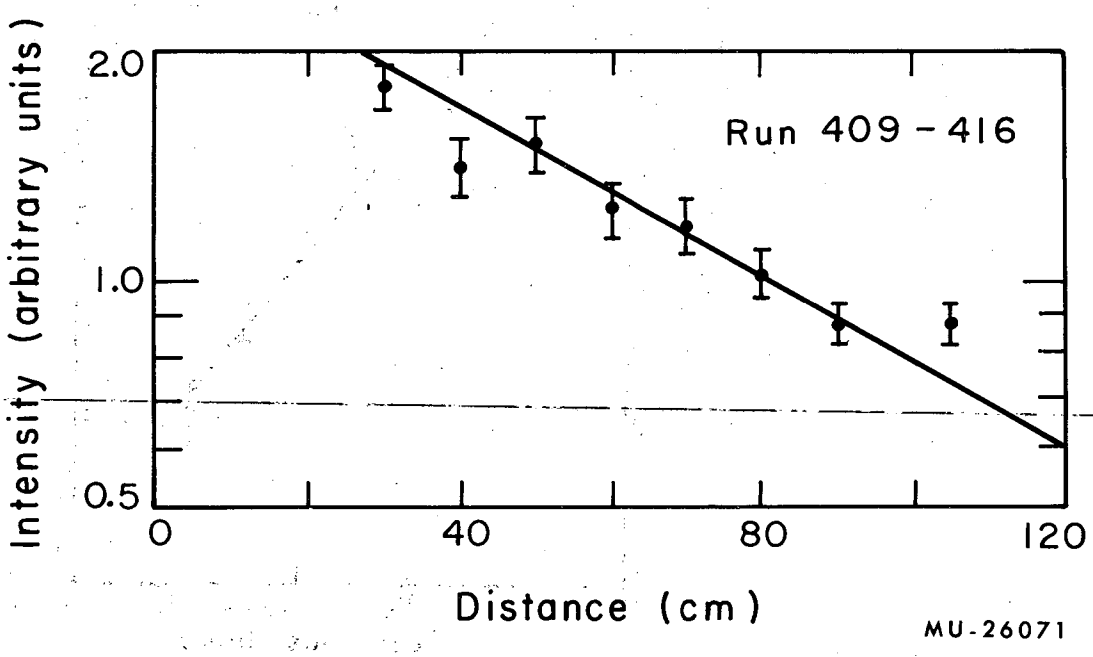

Fig. 12. H atom–H_2 system. Flow H_2, 3.4 cc/min; total pressure, 0.35 mm Hg; surface, quartz.

as the hydrogen atom concentration decreased. This is shown on the graphs by the uncertainties in the positions of the points. The straight lines on the graphs are the best fit to the data and are drawn by eye. The maximum error in the half distance is estimated to be about 15%. On some of the graphs, the initial point is below the line drawn through the other points. This point tends to make the disappearance of H atoms less than first order in H atoms. The reason for the sag of the initial point is not known.

Other data, which are approximately the same as those plotted in the graphs, are given in tabular form, Tables I through IV. Table V gives the experimental parameters and the distances for half reaction of the H atom recombination runs.

2. H in Mixtures of H_2 and O_2

The hydrogen atom - oxygen molecule data were treated in the same way as for the H atom - H_2 system. The logarithm of the intensity of the H atom signal (arbitrary units) vs the distance from the mixing section (cm) was again plotted, and the data appeared to fit a first-order plot. Different runs were made with various O_2 concentrations, and some experiments were run with argon added as a third body.

Figures 13 through 18 are plots of some of the runs. The rest of the data are presented in Tables VI through XXII. The errors in these measurements are of the same source and magnitude as mentioned with the H atom recombination data. Table XXIII gives the experimental parameters and the distances for half reaction. Here $\tau_{1/2}$ is the time for half reaction and is the distance for half reaction divided by the velocity. The other columns in Table XXIII are discussed later.

Table I. Data from run 367-372, H atom-H_2 system. Flow H_2, 4.0 cc/min. Total pressure, 0.26 mm Hg.

Distance (cm)	Intensity (arbitrary units)
30	1.79
40	1.94
60	1.64
80	1.31
100	0.92
110	0.94

Table II. Data from run 396-402, H atom-H_2 system. Flow H_2, 1.3 cc/min. Total pressure, 0.43 mm Hg.

Distance (cm)	Intensity (arbitrary units)
30	3.58
45	2.46
60	2.24
75	1.61
90	1.36
100	.82
110	.55

Table III. Run 258-262, H atom-H_2-A system. Flow H_2, 4.0 cc/min. Flow Ar, 2.4 cc/min. Total pressure, 0.56 mm Hg.

Distance (cm)	Intensity (arbitrary units)
40	1.55
46	1.40
60	1.21
70	1.25
80	1.07

Table IV. Run 388-394, H atom-H_2 system. Flow H_2 4.0 cc/min. Total pressure .85 mm Hg.

Distance (cm)	Intensity (arbitrary units)
30	2.12
45	1.33
60	1.19
75	.90
90	.76
100	.43
110	.33

Table V. H atom - H_2 data and calculated values

Run	Surface	Flow H_2 (cc/min, 1 atm)	Flow Ar (cc/min, 1 atom)	Pressure total (mm Hg)	Distance for half reaction (cm)	Linear of H_2 velocity (cm/sec)	Diameter of cylinder (cm)
251-257	H_3PO_4	4.0		.24	51.3	318	0.92
312-319	Quartz	4.2		.25	47.5	320	0.92
367-372	Quartz	4.0		.26	67.2	293	0.92
345-353	Quartz	5.8		.33	54.0	335	0.92
337-341	Dri Film	6.3		.37	54.0	325	0.92
331-336	Dri Film	6.5		.38	42.0	326	0.92
396-402	Quartz	1.3		.43	32.7	58	0.92
382-387	Quartz	1.5	4.8	.43	55.5	210	0.92
322-330	Quartz	8.1		.45	56.0	343	0.92
258-262	H_3PO_4	4.0	2.4	.56	76.0	218	0.92
388-394	Quartz	4.0		.85	29.8	89.8	0.92
403-408	Quartz	.9		.91	23.8	18.8	0.92
409-416	Quartz	3.4		.35	53.0	302	0.72

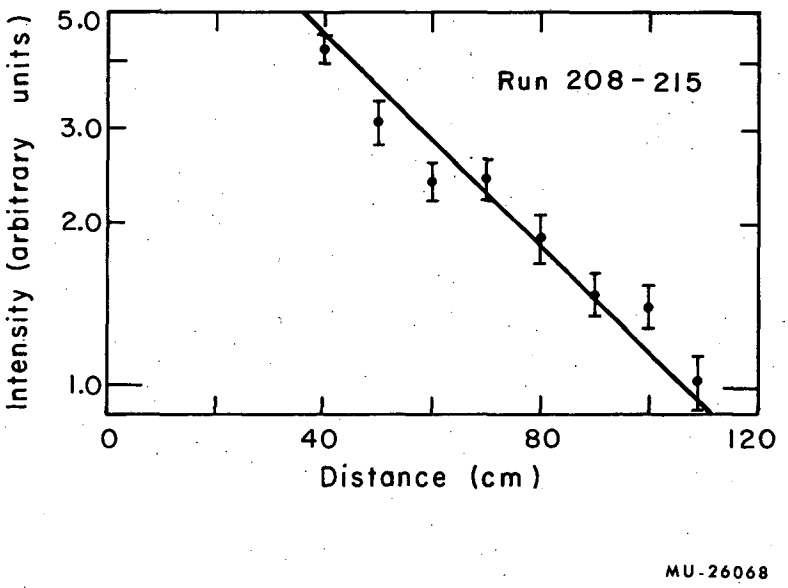

Fig. 13. H atom–H_2-O_2 system. Flow H_2, 4.0cc/min; Flow O_2, 1.1 cc/sec; total pressure, 0.31 mm Hg.

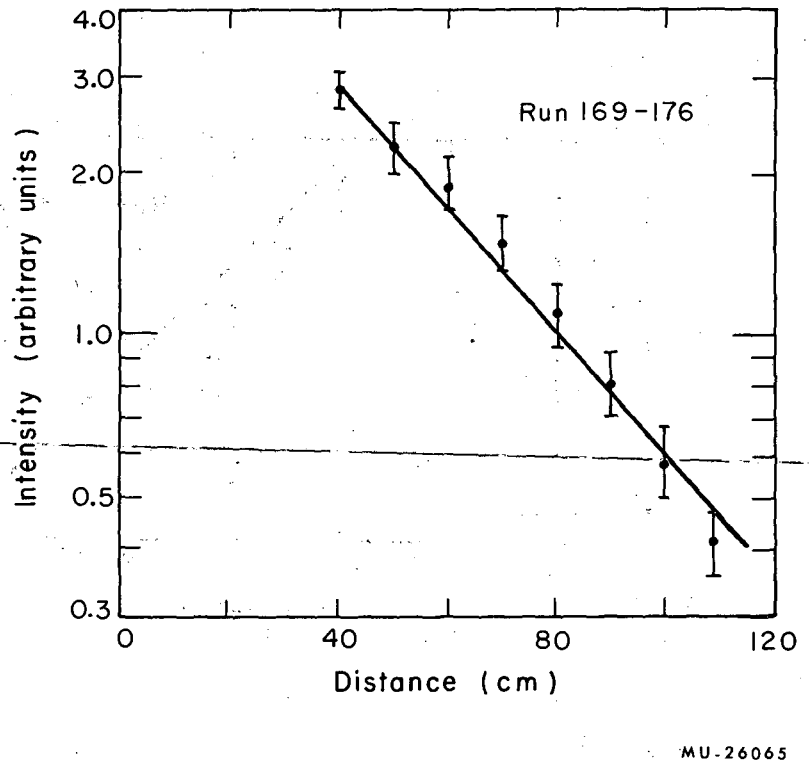

Fig. 14. H atom–H_2-O_2 system. Flow H_2, 3.8 cc/min; Flow O_2, 1.6 cc/min; total pressure, 0.34 mm Hg.

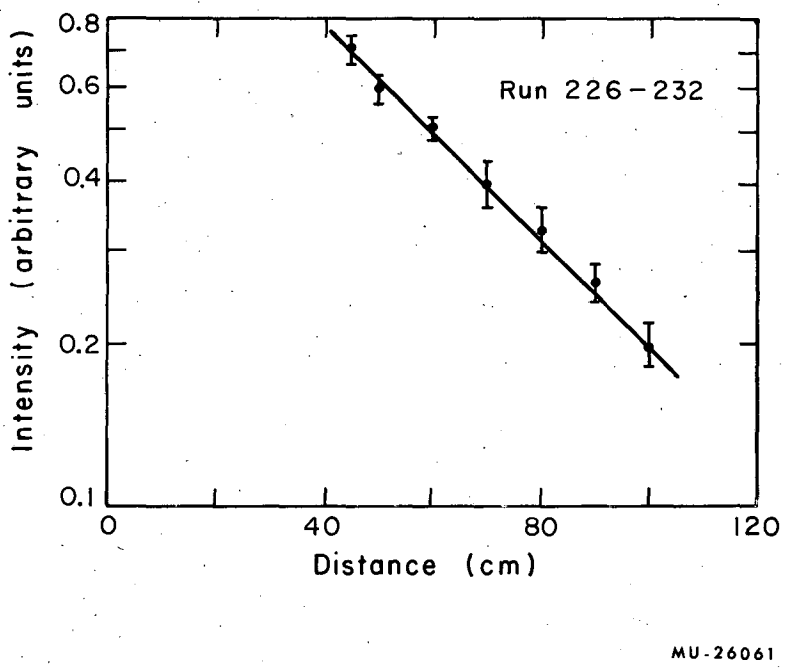

Fig. 15. H atom–H_2-O_2-Ar system. Flow H_2, 3.5 cc/min; Flow O_2, 1.8 cc/sec; Flow Ar, 3.2 cc/sec; total pressure, 0.54 mm Hg.

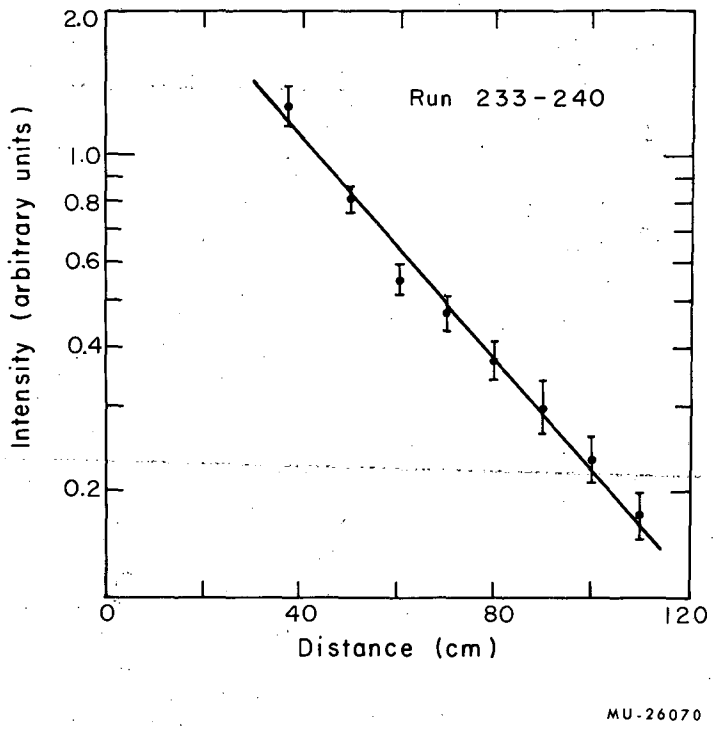

Fig. 16. H atom–H_2-O_2-Ar system. Flow H_2, 3.5 cc/min; Flow O_2, 1.8 cc/min; flow Ar, 0.42 cc/min; total pressure, 0.36 mm Hg.

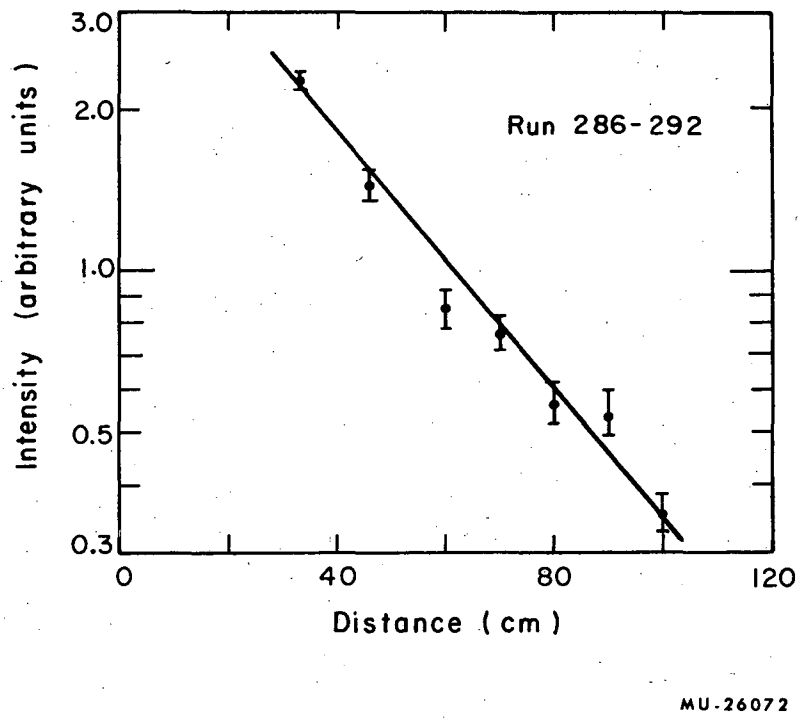

Fig. 17. H atom–H_2-O_2 system. Flow H_2, 5.8 cc/min; flow O_2, 3.4 cc/min; total pressure, 0.51 mm Hg.

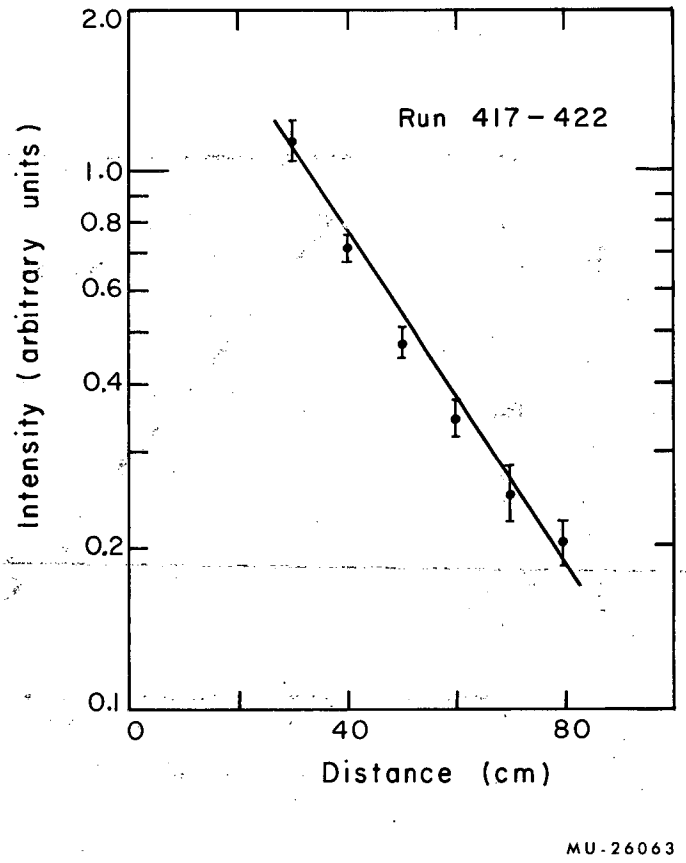

Fig. 18. H atom–H_2-O_2 system. Flow H_2, 3.7 cc/min; flow O_2, 1.5 cc/min, total pressure, 0.46 mm Hg.

Table VI. Run 149-154, H atom - H_2 - O_2 system. Flow H_2, 3.5 cc/min. Flow O_2, 0.7 cc/min. Total pressure, 0.29 mm Hg.

Distance (cm)	Intensity (arbitrary units)
30	10.63
40	13.60
50	10.80
60	10.40
70	8.83
80	6.33

Table VII. Run 161-168, H atom - H_2 - O_2 system. Flow H_2, 4.2 cc/min. Flow O_2, 1.1 cc/min. Total pressure, 0.31 mm Hg.

Distance (cm)	Intensity (arbitrary units)
40	3.04
50	2.72
60	2.29
70	2.33
80	1.64
90	1.17
100	0.90
109	0.89

Table VIII. Run 184-188, H atom - H_2 - O_2 system. Flow H_2 3.8 cc/min. Flow O_2 1.3 cc/min. Total pressure .32 mm Hg.

Distance (cm)	Intensity (arbitrary units)
40	1.82
50	1.52
60	1.28
70	1.13
80	.77

Table IX. Run 143-148, H atom - H_2 - O_2 system. Flow H_2 3.5 cc/min. Flow O_2 1.6 cc/min. Total pressure .34 mm Hg.

Distance (cm)	Intensity (arbitrary units)
30	5.06
40	4.43
50	2.72
60	2.52
70	3.90
80	2.33

Table X. Run 109-114, H atom - H_2 - O_2 system. Flow H_2 4.4 cc/min. Flow O_2 1.6 cc/min. Total pressure .33 mm Hg.

Distance (cm)	Intensity (arbitrary units)
40	2.25
50	1.90
60	1.78
70	1.71
80	1.25

Table XI. Run 200-207, H atom - H_2 - O_2 system. Flow H_2 4.2 cc/min. Flow O_2 2.1 cc/min. Total pressure .37 mm Hg.

Distance (cm)	Intensity (arbitrary units)
40	1.33
50	1.04
60	.71
70	.62
80	.48
90	.33
100	.26
108	.22

Table XII. Run 177-183, H atom - H_2 - O_2 data. Flow H_2 4.2 cc/min. Flow O_2 2.1 cc/min. Total pressure .36 mm Hg.

Distance (cm)	Intensity (arbitrary units)
40	2.22
50	1.67
60	1.05
70	.82
80	.56
90	.46
100	.26

Table XIII. Run 130-135, H atom - H_2 - O_2 data. Flow H_2 4.2 cc/min. Flow O_2 2.2 cc/min. Total pressure .36 mm Hg.

Distance (cm)	Intensity (arbitrary units)
30	1.95
40	1.52
50	1.14
60	.85
70	.81
80	.56

Table XIV. Run 116-119, H atom - H_2 - O_2 data. Flow H_2 4.4 cc/min. Flow O_2 4.2 cc/min. Total pressure .53 mm Hg.

Distance (cm)	Intensity (arbitrary units)
30	.91
40	.57
50	.43
60	.32

Table XV. Run 139-142, H atom - H_2 - O_2 system. Flow H_2 - 4.0 cc/min. Flow O_2 5.2 cc/min. Total pressure .59 mm Hg.

Distance (cm)	Intensity (arbitrary units)
30	.53
40	.29
50	.19
60	.13

Table XVI. Run 216-223, H atom - H_2 - O_2 data. Flow H_2 3.6 cc/min. Flow O_2 1.8 cc/min. Total pressure .32 mm Hg.

Distance (cm)	Intensity (arbitrary units)
40	1.24
50	.81
60	.68
70	.55
80	.44
90	.36
100	.26
109	.21

Table XVII. Run 271-275, H atom - H_2 - O_2 - Ar data. Flow H_2 3.5 cc/min. Flow O_2 4.2 cc/min. Flow Ar 3.35 cc/min. Total pressure .70 mm Hg.

Distance (cm)	Intensity (arbitrary units)
33	1.03
46	.62
60	.47
70	.31
80	.22

Table XVIII. Run 276-279, H atom - H_2 - O_2 data. Flow H_2 3.6 cc/min. Flow O_2 4.2 cc/min. Total pressure .52 mm Hg.

Distance (cm)	Intensity (arbitrary units)
33	.78
46	.39
60	.28
70	.21

Table IXX. Run 280-285, H atom - H_2 - O_2 data. Flow H_2 3.3 cc/min. Flow O_2 2.6 cc/min. Total pressure .40 mm Hg.

Distance (cm)	Intensity (arbitrary units)
33	1.28
46	.82
60	.47
70	.43
80	.26
90	.23

Table XX. Run 301-308, H atom - H_2 - O_2 data. Flow H_2 5.8 cc/min. Flow O_2 1.22 cc/min. Total pressure .40 mm Hg.

Distance (cm)	Intensity (arbitrary units)
33	1.75
46	1.49
60	1.26
70	1.15
80	1.03
90	.96
100	.63
110	.61

Table XXI. Run 423-428, H atom - H_2 - O_2 data. Flow H_2 3.1cc/min. Flow O_2 .9 cc/min. Total pressure .36 mm Hg.

Distance (cm)	Intensity (arbitrary units)
30	1.77
40	1.33
50	.94
60	.65
70	.55
80	.42

Table XXII. Run 429-433, H atom - H_2 - O_2 data. Flow H_2 6.2 cc/min. Flow O_2 1.8 cc/min. Total pressure .62 mm Hg.

Distance (cm)	Intensity (arbitrary units)
30	1.48
40	1.18
50	.61
60	.60
70	.29

Table XXIII. H atom - H_2 - O_2 data and calculated values

Run	Flow H_2 (cc/min) 1 atm.	Flow O_2 (cc/min) 1 atm.	Flow Ar (cc/min) 1 atm.	Pressure Total (mm Hg)	Distance for half reaction (cm)	Linear velocity H_2 (cm/sec)
149-154	3.5	.7		.29	37.5	279
161-168	4.2	1.1		.31	32.5	320
208-215	4.0	1.1		.31	33.5	318
184-188	3.8	1.3		.32	39.3	302
143-148	3.5	1.6		.34	42.7	290
109-114	4.4	1.6		.33	41.0	349
169-176	3.8	1.6		.34	26.1	302
200-207	4.2	2.1		.37	26.0	320
177-183	4.2	2.1		.36	19.6	333
130-135	4.2	2.2		.36	27.5	334
116-119	4.4	4.2		.53	20.5	311
139-142	5.2	5.2		.59	14.9	293
216-223	3.6	1.8		.32	27.6	326
226-232	3.5	1.8	3.2	.54	29.8	304
233-240	3.5	1.8	.42	.36	26.4	304
271-275	3.5	4.2	3.35	.70	21.7	304
276-279	3.6	4.2		.52	18.0	286
280-285	3.3	2.6		.40	21.1	286
286-292	5.8	3.4		.51	25.2	345
301-308	5.8	1.22		.40	55.4	336
417-422	3.7	1.5		.46	18.3	348
423-428	3.1	.9		.36	23.3	344
429-433	6.2	1.8		.62	18.8	401

(continued)

Table XXIII - (continued)

Run	Diameter Cylinder (cm)	$\tau_{1/2}$ x 10 sec	$\tau'_{1/2}$ x 10 sec	$\tau'_{1/2}(O_2)$ x 10^2 (mm Hg sec)	$\frac{\tau'_{1/2}(O_2)}{P}$ x 10^2 T sec
149-154	0.92	1.34	3.2	1.6	.55
161-168	0.92	1.02	1.6	.96	.31
208-215	0.92	1.05	1.8	1.3	.41
184-188	0.92	1.30	3.7	3.0	.93
143-148	0.92	1.51	7.6	7.6	2.2
109-114	0.92	1.17	3.3	3.0	.90
169-176	0.92	.86	1.3	1.3	.38
200-207	0.92	.81	1.1	1.3	.35
177-183	0.92	.58	.59	.71	.20
130-135	0.92	.82	1.2	1.0	.28
116-119	0.92	.66	.84	2.2	.42
139-142	0.92	.51	.53	1.8	.30
216-223	0.92	.85	1.2	1.3	.41
226-232	0.92	.98	2.1	2.3	.43
233-240	0.92	.87	1.2	1.3	.37
271-275	0.92	.71	1.1	3.0	.42
276-279	0.92	.63	.73	2.0	.39
280-285	0.92	.74	.88	1.6	.40
286-292	0.92	.73	1.1	2.1	.41
301-308	0.92	1.65	-	-	-
417-422	0.72	.53	.60	.78	.24
423-428	0.72	.68	.89	.71	.20
429-433	0.72	.47	.58	.81	.13

III. DISCUSSION

A. H in H_2

In the pressure range used in these experiments, heterogeneous reaction at the walls is an important process for the recombination of the atoms. Previous work, as described in the introduction to this thesis has shown that this is a process of first order in H atoms. Homogeneous second-order recombination in the gas phase would be an important mechanism at higher pressures. Since the experimental data seemed to fit a first-order plot reasonably well, it was decided to try to fit the data with a mechanism which employed destruction of the atoms at the walls. The treatment was based on a mathematical model similar to that of Wise and Ablow.[19,21]

The model assumed that H atoms were lost on the surface of an infinitely long cylinder. This loss is expressed by the recombination coefficient γ, which is defined as the ratio of the number of atoms striking and reacting with the surface to the total number of atoms striking the surface. Following the notation of Wise and Ablow, γ is expressed in terms of the dimensionless constant δ, given by $\delta = 4D/\gamma cR$, for $\gamma << 1$. D is the diffusion coefficient of H atoms in H_2, or -- in the third-body experiments (addition of Ar) -- D is the diffusion coefficient of H atoms in the mixture of gases. The units of D are cm^2/sec. The rms speed of H atoms is c, expressed in units of cm/sec, and R (in cm) is the radius of the cylinder. The equation employed in our analysis is a modification of Fick's second law of diffusion. Before the derivation is given a short discussion of Fick's first and second laws of diffusion is in order. For a fuller and more rigorous discussion see Crank.[26]

The fundamental hypothesis in the theory of diffusion is that the rate of transfer of a diffusing substance per unit area F is proportional to the concentration gradient measured normal to the unit area,

$$F_x = -D \frac{\partial n}{\partial x}, \tag{1}$$

where D is the proportionality constant and is called the diffusion coefficient, n is the concentration of the diffusing substance, and x is the coordinate normal to the unit area. The minus sign arises because the direction of flow is opposite to that of increasing concentration. This hypothesis holds only for isotropic media, and may be generalized to three dimensions by writing down the corresponding terms in the y and z directions.

Let us consider two parallel planes of unit area which bound a volume element whose length is dx. Then the increase per unit time of the concentration within this volume bounded by x on one side and x+dx on the other side is

$$F_x - F_{x+dx} = D(-\partial n/\partial x)_x + (\partial n/\partial x)_{x+dx}),$$

by Eq. (1). After dividing through the above equation by dx, and since we have

$$(\partial n/\partial x)_{x+dx} = (\partial n/\partial x)_x + (\partial/\partial x)(\partial n/\partial x)\, dx,$$

the increase of concentration with time is

$$\partial n/\partial t = D(\partial^2 n/\partial x^2). \tag{2}$$

Equations (1) and (2) and Fick's first and second laws of diffusion,[27] and were first discovered by analogy with Fourier's equations of heat conduction. The above equations have been derived by assuming D is constant.

Generalizing Eq. (2) to three dimensions, we find

$$\partial n/\partial t = D\,(\partial^2 n/\partial x^2 + \partial^2 n/\partial y^2 + \partial^2 n/\partial z^2). \qquad (3)$$

Since our model is for a cylinder, we transform Eq. (3) into cylindrical coordinates. Let

$$x = r\cos\theta,\ y = r\sin\theta,\ z = z.$$

Substituting into Eq. (3), one gets

$$\partial n/\partial t = \frac{D}{r}\left\{\frac{\partial}{\partial r}\left(r\frac{\partial n}{\partial x}\right) + \frac{\partial}{\partial\theta}\left(\frac{1}{r}\frac{\partial n}{\partial\theta}\right) + \frac{\partial}{\partial z}\left(r\frac{\partial n}{\partial z}\right)\right\}.$$

Since in this problem $(\partial n/\partial\theta) = 0$, this reduces to

$$\partial n/\partial t = D\left[\frac{1}{r}\frac{\partial}{\partial r}\left(r\frac{\partial n}{\partial r}\right) + \frac{\partial^2 n}{\partial z^2}\right].$$

This is Fick's second law in cylindrical coordinates.

The equation we use to analyze our data is

$$\partial n/\partial t = D\left[\frac{1}{r}\frac{\partial}{\partial r}\left(r\frac{\partial n}{\partial r}\right) + \frac{\partial^2 n}{\partial x^2}\right] - v\frac{\partial n}{\partial x}, \qquad (4)$$

where x is the coordinate along the axis of the cylinder which we previously called z, r is the radial coordinate, n is the concentration of H atoms, and v is the velocity of gas flow in the x direction.

Equation (4) has an extra term added to Fick's second law ($-v\,\partial n/\partial x$) to account for the fact that diffusion is occurring in a flowing system. The reaction studied took place under steady-state conditions, so that we have

$$\partial n/\partial t = 0,$$

and Eq. (4) becomes

$$D\left[\frac{1}{r}\frac{\partial}{\partial r}\left(r\frac{\partial n}{\partial r}\right) + \frac{\partial^2 n}{\partial r^2}\right] - v\frac{\partial n}{\partial x} = 0. \qquad (5)$$

The following boundary conditions applied to this equation are

$$n(r,\ x = 0) = n_o, \qquad (6)$$

$$\partial n/\partial r(r=0,x) = 0, \tag{7}$$

$$n(r,\ x = \infty) = 0, \tag{8}$$

$$\partial n/\partial r(r = R,\ x) = -n(R,x)/\delta R. \tag{9}$$

Equation (6) defines the number of H atoms at x = 0. Equation (7) defines the concentration along the axis of the cylinder as a maximum. Equation (8) gives the concentration of H atoms at infinity which is (zero), and Eq. (9) defines the number lost on the cylinder walls.[28]

As shown in Appendix 1, the solution of Eq. (5) consists of separating it into two parts, the radial part and the linear part. Each part can then be solved separately. For the conditions we are interested in ($\gamma \ll 1,\ \delta \gg 1$),[15] the radial part reduces to a constant. This means that there is no concentration gradient in the radial direction. Therefore the solution of Eq. (5) is

$$n/n_o = \exp\left\{1/2\left[\frac{v}{D} - \left(\frac{v^2}{D^2} + \frac{2\gamma C}{DR}\right)^{1/2}\right]x\right\}, \tag{10}$$

and is the solution of the linear part of the differential equation multiplied by a constant.

From the experimental data we found the distance for half reaction, $d_{1/2}$. Using an equation similar to Eq. (10), we see

$$n/n_o = \exp(-kx),$$

$$0.5 = \exp(-kd_{1/2}),$$

$$-k = -.693/d_{1/2} = 1/2\left(\frac{v}{D} - \left[\frac{v^2}{D^2} + \frac{2\gamma C}{DR}\right]^{1/2}\right),$$

and

$$\gamma = (k^2D + kv)\ 2R/c. \tag{11}$$

Equation (11) has two parameters that can be determined by experiments

at different flow rates. These parameters are D and γ. Amdur has given a value for D (for H atoms in H_2) which is $D = 1.4 \times 10^3/P$ (in mm Hg) cm^2/sec.[29] Recently, Collins and Hutchins determined D by electron paramagnetic resonance experiments and found it to be $(2.0^{+}_{-} .2) \times 10^3/P$ (mm Hg) cm^2/sec.[30] In Table XXIV values of γ are presented for various values of D.

Table XXIV shows that no one particular value of D increases markedly the agreement of the values of γ per column. The reason for this is that in our system, as the pressure increases, the flow and the diffusion coefficient decrease and k increases. These changes tend to compensate each other and the value of γ remains nearly the same. Values for γ calculated from the larger values of the diffusion coefficient agree slightly better. The data indicate that Amdur's values of the diffusion is too low. For the H atom - O_2 measurements described in the next section we use $D = 2.0/P$ (mm Hg) cm^2/sec and $\gamma = 1.8 \times 10^{-5}$.

The values of γ found in our work vary from 0.9×10^{-5} to 2.5×10^{-5}. Collins and Hutchins determined γ for a pyrex surface treated with hydrofluoric acid, and found it to be $0.7 \pm .1 \times 10^{-5}$.[30] Smith reported a value of $\gamma = 1.05 \times 10^{-5}$ for a clean pyrex surface.[15] Poole found a value for γ of 1.6×10^{-4}.[16] Steiner's values for γ ranged from 2×10^{-6} to 9×10^{-6}.[18] Smith's experiments were similar to ours except that he used a catalytic probe to analyze for H atoms. Steiner's and Poole's values for γ were calculated from work in which surface recombination was a minor effect. Our values of γ are in the same range as the earlier direct measurements, and show that our methods of measurement and calculation give reasonable results.

Table XXIV. Values of γ for various values of the diffusion coefficient.

$D\left(\frac{cm^2}{sec}\right)$	$\frac{1.4 \times 10^3}{P(mm\ Hg)}$	$\frac{2.0 \times 10^3}{P(mm\ Hg)}$	$\frac{3.0 \times 10^3}{P(mm\ Hg)}$
Run	$\gamma \times 10^5$	$\gamma \times 10^5$	$\gamma \times 10^5$
251-257	2.0	2.1	2.4
312-319	2.2	2.3	2.7
367-372	1.3	1.4	1.6
345-353	1.8	1.9	2.1
337-341	1.8	1.9	2.0
331-336	2.4	2.5	2.8
396-402	1.0	1.2	1.6
382-387	1.1	1.2	1.2
322-330	1.7	1.8	1.9
258-262	1.4	1.5	1.6
388-394	1.1	1.2	1.5
403-408	.7	.9	1.2
409-416	1.3	1.4	1.6
Average	$1.5 \pm .4$	$1.6 \pm .4$	$1.9 \pm .4$
Average (not including Run 403-408)	$1.6 \pm .4$	$1.7 \pm .4$	$1.9 \pm .4$

B. H in Mixtures of H_2, O_2, and A

1. Calculations

The H atom - O_2 data fitted a first-order plot, and the over-all rate of consumption of H atoms was higher in this system than in the H atom - H_2 recombination work. This shows that another reaction besides H atom surface recombination consumed H atoms and that it is of first order in H atoms. This is the reaction of H atoms and O_2 molecules. In order to account quantitatively for this first-order reaction another term was added to the diffusion equation.

The modified equation is

$$D\left[\frac{1}{r}\left(r\frac{\partial n}{\partial r}\right)+\frac{\partial^2 n}{\partial x^2}\right]-v\frac{\partial n}{\partial x}-k_1 n=0 \qquad (12)$$

where all symbols are the same as before except for D, which is now the diffusion coefficient for H atoms in mixtures of H_2, O_2, and Ar.

In this equation, k_1 is the first-order rate constant for the disappearance of H atoms. The solution of Eq. (12) is very similar to the solution of Eq. (5), and is also shown in Appendix 1. The boundary conditions for Eq. (12) are the same as for Eq. (5).

The solution for Eq. (12) is

$$n/n_o = \exp\left\{1/2\left[\frac{v}{D}-\left(\frac{v^2}{D^2}+\frac{4k_1}{D}+\frac{2\gamma C}{DR}\right)^{1/2}\right]x\right\}. \qquad (13)$$

As shown in the previous section the experimental quantity obtained is $d_{1/2}$, so that we have

$$n/n_o = \exp\left(-k_o d_{1/2}\right),$$

$$k_o = 0.693/d_{1/2} = 1/2. \qquad (14)$$

Solving for k_1, we find

$$k_1 = Dk_o^2 + k_o v - \gamma c/2R. \qquad (15)$$

The only change made in the system has been the addition of O_2, therefore k_1 is the first-order rate constant for the reaction of H atoms with O_2. Since k_o, the experimental rate constant, is determined by two simultaneous reactions, which are the reaction of H + O_2 and the recombination of H atoms on the walls, then $k_o \geqslant k_1$, the rate constant for the H + O_2 reaction alone. If we call $\tau_{1/2}$ the experimental half life ($\tau_{1/2} = d_{1/2}/v = 0.693/k_o$) and $\tau'_{1/2}$ the half life for the reaction of H atoms with O_2. ($\tau'_{1/2} = 0.693/k_1$), we have $\tau'_{1/2} \geqq \tau_{1/2}$.

We can now calculate k_1 and $\tau'_{1/2}$. The value of γ used is 1.9×10^{-5} which was found from the H atom recombination work. By assuming that the diffusion coefficient of H atoms in O_2 is equal to the diffusion coefficient of H atoms in Ar, we can use the data of Wise[31] to determine the diffusion coefficient of H atoms in the mixture H_2, O_2 and Ar. Values for $\tau_{1/2}$ and $\tau'_{1/2}$ are given in Table XXIII. Comparing the values of $\tau'_{1/2}$ and $\tau_{1/2}$, we see that at low O_2 concentrations the H atom recombination reaction is very important, but as the O_2 concentration increases the importance of H atom recombination diminishes until at high O_2 concentrations it is of little significance.

The last columns in Table XXIII show the values obtained when $\tau'_{1/2}$ is first multiplied by the O_2 concentration and then the product is divided by the total pressure. Since almost any simple mechanism gives the reaction of H + O_2 as first order in O_2, we would expect $\tau'_{1/2}(O_2)$ multiplied by or divided by some function of the total

pressure to be equal to a constant. As can be seen from the last column in Table XXIII, $\tau'_{1/2}(O_2)/P_{total}$ is nearly constant for most of the runs. In Fig. 19 a plot of $\tau'_{1/2}(O_2)$ vs P_{total} shows the general scatter of these data. The data for the smaller tube (d = 0.72 cm) do not fit this plot. The above relationship means that any reaction mechanism written to explain the rate of decay of H atoms will have to be a first-order process with respect to O_2 and inversely proportional to the total pressure. The deviation of the data for the smaller tube will also have to be explained.

2. Mechanisms

Various reaction mechanisms have been proposed for the H + O_2 reaction. Burgess and Robb, whose experiments were run at total pressures higher than ours, proposed a mechanism.[13] Their mechanism contains a chain reaction, which will not be important at our low pressures, but it does show that the rate of disappearance of H atoms is directly proportional to the total pressure. The primary steps in their reaction mechanism are

$$H + O_2 \xrightarrow{k_a} HO_2^*, \qquad (a)$$

$$HO_2^* \xrightarrow{k_b} H + O_2, \qquad (b)$$

$$HO_2^* \xrightarrow{k_m} HO_2, \qquad (m)$$

so that one has

$$-d(H)/dt \approx k_m k_a (H)(O_2)(M)/k_b,$$

assuming steady state for HO_2^*. Meyer used steps (a) and (b), but postulated for the last step[3]

$$HO_2^* \xrightarrow{k_c} HO_2 + h\nu, \qquad (c)$$

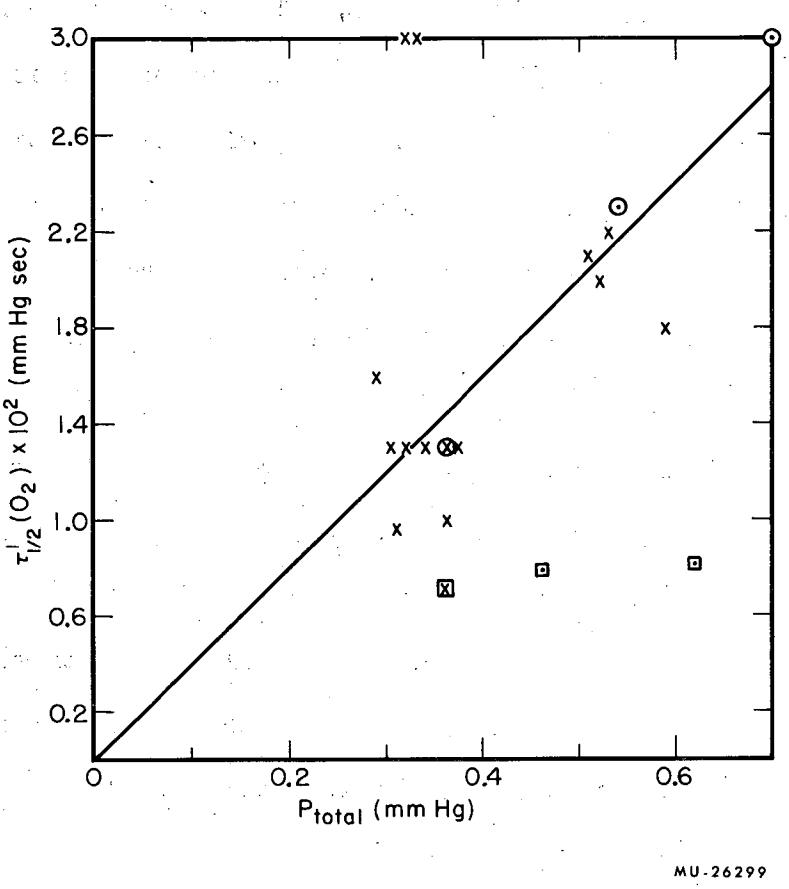

Fig. 19. $\tau_{1/2}'(O_2)$ vs P_{total}.

giving

$$-d(H)/dt \approx k_c k_a (H)(O_2)/k_b .$$

In his mechanism the total pressure had no effect on the rate of disappearance of the H atoms. Neither of these mechanisms can explain our data.

A possible mechanism to explain our results is

$$H + O_2 \xrightarrow{k_a} HO_2^*, \qquad (a)$$

$$HO_2^* \xrightarrow{k_b} H + O_2, \qquad (b)$$

$$HO_2^* + \text{Wall} \xrightarrow{k_w} HO_2 + \text{wall}, \qquad (w)$$

$$HO_2 + H \xrightarrow{k_d} 2OH, \qquad (d)$$

$$H + OH + M \xrightarrow{k_f} HOH + M, \qquad (f)$$

where the last two steps have been added to show the ultimate fate of HO_2 and to explain the production of OH. The rate of reaction of H atoms in this mechanism, assuming steady state for HO_2^*, HO_2, and OH, is

$$-d(H)/dt = 4k_w k_a (H)(O_2)/(k_b + k_w). \qquad (15)$$

In this expression the steady-state assumptions for HO_2 and OH do not change the form of the equation, but only produce a numerical factor of four. Under the conditions of a relatively slow over-all reaction, $k_b \gg k_w$, so that this mechanism gives

$$-d(H)/dt = 4k_w k_a (H)(O_2)/k_b .$$

Under our conditions k_w is pressure-dependent, so that the rate of disappearance of H atoms is inversely proportional to the total pressure. The rate constant for the deactivation of HO_2^* at the surface of the cylindrical tube is k_w. If we assume that HO_2^* is deactivated on the

walls very efficiently, then the magnitude of k_w depends on the diffusion coefficient of HO_2^* and hence on the total pressure. This means that γ, the ratio of the number of collisions that deactivate the molecule to the total number of collisions, is approximately unity. If the surface were inefficient ($\gamma < 10^{-2}$) there would be no concentration gradient of HO_2^* in the reaction tube and therefore no pressure dependence. This effect was shown earlier in the H atom recombination work. The problem of calculating surface destruction constants in cylindrical vessels has been quantitatively treated by Semenoff.[32] For surfaces of high efficiency the first calculations were done by Bursian and Sorokin.[33] Recently Baldwin has taken Semenoff's results and has extended them over a wide range of γ.[34]

The following diffusion equation has been solved for n, the number of reacting species under steady-state conditions:

$$D \frac{\partial^2 n}{\partial r^2} + \frac{D}{r} \frac{\partial n}{\partial r} + (f-g)\, n + n_o = \frac{\partial n}{\partial t} = 0. \qquad (16)$$

This equation has been derived for chain reactions, and the nomenclature is taken from this type of reaction (see Baldwin):

f = gas-phase branching constant (in our case f = 0),

g = gas-phase termination constant,

n_o = initiation rate per unit volume.

Under steady-state conditions

$$n_s = n_o/(k_s + g - f), \qquad (17)$$

where k_s = surface termination constant.

For our mechanism, assuming steady state, we have

$$HO_2^* = k_a(H)(O_2)/(k_b + k_w), \qquad (18)$$

therefore $n_o = k_1(H)(O_2)$, $g = k_b$, $f = 0$, and $k_s = k_w$.

Baldwin has sketched the method of solution for this diffusion equation, and gives in his paper a table for the solution under various conditions of total pressure and γ.

For $\gamma \approx 1$,

$$k_s \text{ (or } k_w) = 5.8\ D/r^2. \tag{19}$$

For the detailed mathematical solution of this diffusion equation, refer to Semenoff. We use Baldwin's expanded treatment of this problem.

In order to use the above equation to calculate k_w, the diffusion coefficient of HO_2^* in a mixture of H_2 and O_2 (assuming O_2 and Ar are the same) can be approximated from the diffusion coefficient of N_2 in H_2 and O_2. The true diffusion coefficient for HO_2^* is probably less than the one we calculate, but because of the lack of data we use the above approximation. The diffusion coefficient of CO and CO_2 in O_2 differ by about 25%.[35] The diffusion coefficient of HO_2^* in H_2 and in O_2 would probably differ by less than this amount from the diffusion coefficient of N_2 in H_2 and O_2.

From tables in Hirschfelder, Curtiss, and Bird[35] we find that at 1 atmosphere and 293°K the diffusion coefficient of N_2 in H_2 is 0.76 cm^2/sec and the diffusion coefficient of N_2 in O_2 is 0.22 cm^2/sec. Then we can use Wilke's formula for interdiffusion coefficient,[36]

$$D_{N_2 \text{ in } H_2,\ O_2} = \left(\frac{n_{H_2}}{D_{N_2 \text{ in } H_2}} + \frac{n_{O_2}}{D_{N_2 \text{ in } O_2}}\right)^{-1} \tag{20}$$

where n_{H_2} and n_{O_2} are the mole fractions of H_2 and O_2 respectively.

From Eq. (15),

$$\frac{-dH}{dt} = \frac{4k_a k_w (H)(O_2)}{k_b + k_w} = k_{exp}(H) = \frac{0.693(H)}{\tau'_{1/2}} .$$

Now, for $k_b \gg k_w$,

$$\frac{4k_a k_w}{k_b} = \frac{0.693}{\tau'_{1/2}(O_2)} .$$

Assuming $\gamma \approx 1$, $k_w = 5.8\ D/R^2$, we have

$$\frac{4x5.8k_a}{r^2 k_b} = \frac{0.693}{\tau'_{1/2}(O_2)D} . \qquad (21)$$

This equation shows that $\tau'_{1/2}(O_2)D$ should be a constant for all the runs. Table XXV lists the individual runs and $\tau'_{1/2}(O_2)D$ for each of them. Figure 20 is a graph of $\tau'_{1/2}(O_2)D$ vs $1/D_{HO_2^*}$. $\tau'_{1/2}(O_2)$ for the smaller tube was normalized to the larger tube by multiplying the values by $(0.92/0.72)^2$, which is the square of the ratio of the radii. Equation (20) shows that this will normalize the $\tau'_{1/2}(O_2)$ values. The average value from Fig. 20 for $\tau'_{1/2}(O_2)D = 1.0 \times 10^1$ cm^2 mm Hg. Assuming $k_a = 3.2x10^9$ sec^{-1} (Burgess and Robb's value), we can now calculate k_b from Eq. (20). We find $k_b = 2.8x10^9$ sec^{-1} for a value of $\gamma \approx 1$. If we assume $\gamma = 0.1$ (using Baldwin's tables), we find $k_b = 1.5x10^9$ sec^{-1}. Baldwin has shown that for the range of pressures of our experiments $\gamma < 0.1$ does not give effective diffusion control of the surface reaction.

The reciprocal of k_b is the lifetime of HO_2^*. Whether HO_2^* is in the ground electronic state or an excited electronic state, it is certainly in an excited vibrational state. The minimum lifetime of an excited electronic state is approximately 10^{-8} sec. The rate-determining step in the decomposition of HO_2^* is the time that the vibrationally

Table XXV. Diffusion coefficient parameter and calculated values.

Run	$\tau_{1/2}(O_2)\times10^2$ (sec mm Hg)	$D_{HO_2^*}\times10^2$ (cm^2/sec)	$D_{HO_2^*}\,\tau_{1/2}(O_2)\times10^{-1}$ (cm^2 mm Hg)	$1/D_{HO_2^*}\times10^3$ (cm^2/sec)$^{-1}$
149-154	1.6	13.96	2.2	.730
161-168	.96	12.52	1.2	.800
208-215	1.3	11.94	1.6	.838
169-176	1.3	10.00	1.3	1.00
200-207	1.3	8.78	1.4	1.14
177-183	.71	8.89	.63	1.13
130-135	1.0	8.89	.89	1.13
116-119	2.2	4.94	1.1	2.02
139-142	1.8	4.12	.74	2.43
216-223	1.3	9.84	1.3	1.02
226-232	2.3	4.35	1.0	2.30
233-240	1.3	8.19	1.1	1.22
271-275	3.0	3.07	.92	3.26
276-279	2.0	4.81	.96	2.08
280-285	1.6	6.88	1.1	1.45
286-292	2.1	5.98	1.3	1.67
417-422	1.3*	7.43	.97	1.35
423-428	1.2*	10.42	1.3	.96
429-433	1.3*	5.97	.78	1.68
			Av. 1.1	

* Normalized to diameter .92 cm.

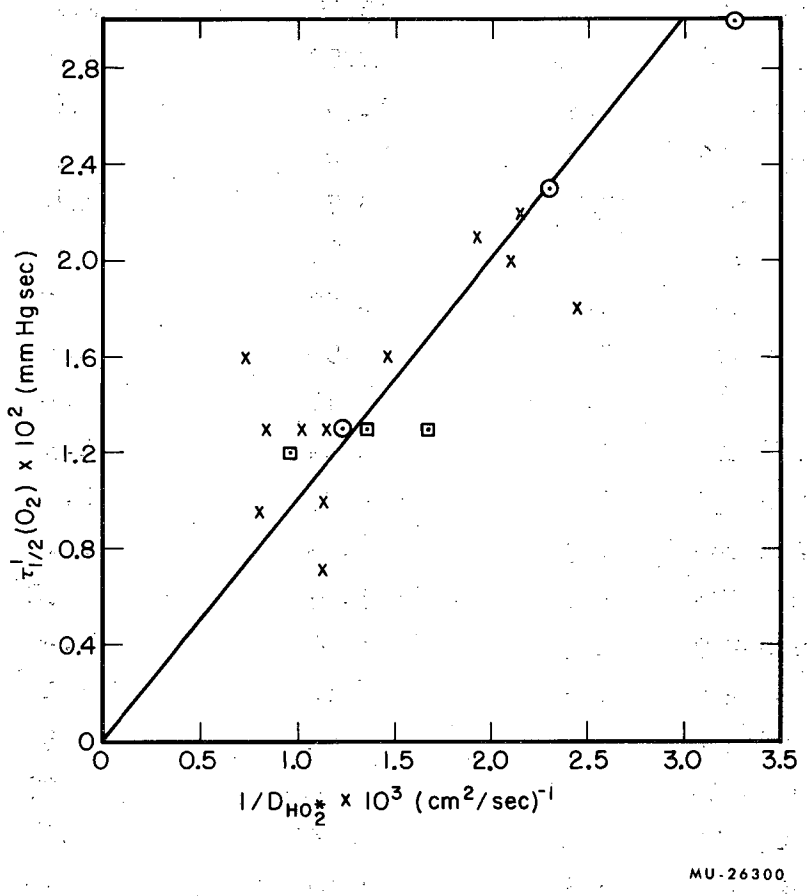

Fig. 20. $\tau_{1/2}'(O_2)$ vs $1/D_{H_2O^*}$.

excited molecule stays in a bounded state. The period for a vibration is about 10^{-12} to 10^{-14} sec. Robertson calculated the lifetime of HO_2^* from his data and found it to be about 5×10^{-12} sec. Meyer found that by assuming a value of 1×10^{-11} sec he could quantitatively explain his OH data. Burgess and Robb found the lifetime of HO_2^* to be 4×10^{-9} sec. Our value of the lifetime of HO_2^* is $(5\pm2)\times10^{-10}$ sec. This lifetime indicates that the 45 kcal of excitation energy[3] of HO_2^* are well distributed through all the molecular vibrations of the molecule.

Our value of the lifetime of HO_2^* is quite reasonable if one considers the complexity of this excited species. This work represents a fairly direct measurement of this lifetime. It is in reasonable agreement with the lifetimes of about 10^{-10} sec found for other vibrationally excited triatomic molecules formed by bimolecular collisions.[37]

3. OH Concentration

By the use of the mechanism written in the previous section, we can solve for OH in steady-state concentration,

$$(OH) = k_a k_w (O_2)/k_f(k_b + k_w)\,(M) \approx k_a k_w (O_2)/k_f k_b (M). \qquad (22)$$

This equation shows that OH should be proportional to the O_2 concentration and approximately inversely proportional to the square of the total pressure. Meyer's data qualitatively followed this dependence except that at higher O_2 pressures the OH concentration increased only slowly with an increasing partial pressure of O_2.

In order to explain the above O_2 dependence, a mechanism is needed that will limit the amount of OH formed. A possible reaction is

$$HO_2 + OH \xrightarrow{k_e} HOH + O_2. \qquad (e)$$

This reaction was also proposed by Meyer. Using this reaction in our

reaction mechanism, together with the values of the rate constants given in the introduction (except for $k_w = k_s = 5.8D/R^2$), we find

$$[OH]_{\text{steady state}} = k_d(D)/2k_e\left[\left(1 + \frac{8k_a k_w k_e(O_2)}{k_b k_d k_f(H)(M)}\right)^{1/2} - 1\right]. \quad (23)$$

This equation shows that at low O_2 concentrations the OH concentration is directly proportional to the O_2 concentration (at constant pressure), but as the O_2 concentration increases the OH concentration becomes proportional to the square root of the H atom concentration and the O_2 concentration. This equation qualitatively explains Meyer's results.

It should be noted that the mechanism discussed previously is just one possible mechanism. The reason it was chosen is that it is the simplest one that fits the data in this thesis and the data in the literature. The reaction step added to explain Meyer's data is quite improbable at low OH and HO_2 concentrations. At low pressures, OH or HO_2 reacting with the walls might be an important termination step. This sort of reaction has been shown in this thesis to be important in the recombination of H atoms and also in the deactivation of HO_2^*.

4. Future Experiments

An interesting experiment would be to raise the total pressure to the point at which collisional deactivation would become important. In this case the pressure dependence of the disappearance of H atoms would change from being inversely proportional to the total pressure to being directly proportional to total pressure. Another method of increasing the collisional deactivation of HO_2^* would be to increase the diameter of the tube. As shown previously, the diffusion coefficient decreases as the square of the radius. With the present apparatus these experi-

ments are difficult to do. But with a lower-frequency electron spin resonance spectrometer it would be possible to increase the diameter of the tube. At the same time it might be possible to raise the total pressure and thereby greatly increase the probability of gas-phase collisional deactivation of HO_2^*.

Acknowledgments

I am very grateful to Professor Rollie J. Myers for his constant advice and encouragement throughout the course of this work.

I would also like to thank Professor Bruce Mahan for some very enlightening conversations.

This work was done under the auspices of the United States Atomic Energy Commission.

Appendix 1

The equation* we wish to solve is

$$D\left[\frac{1}{r}\frac{\partial}{\partial r}\left(r\frac{\partial n}{\partial r}\right)+\frac{\partial^2 n}{\partial x^2}\right]-v\frac{\partial n}{\partial x}=0. \tag{A-1}$$

A solution of this equation is

$$n=\Sigma\, x(r)\,R(r), \tag{A-2}$$

where each term of this series is a solution of (A-1).

Substituting Eq. (A-2) in (A-1), we see

$$R''(r)\,X(x)+\frac{1}{r}R'(r)\,X(x)=X''(x)\,R(r)+\frac{v}{D}\,X'(x)\,R(r).$$

Dividing through by $R(r)\,X(x)$, we have

$$\frac{R''(r)}{R(r)}+\frac{1}{r}\,\frac{R'(r)}{R(r)}=\frac{-X''(x)}{X(x)}+\frac{v}{D}\,\frac{X'(x)}{X(x)}=-K^2, \tag{A-3}$$

where we have now separated the variables and set each side equal to a constant, $-K^2$. We can now solve the linear part and radial part of Eq. (A-3) separately.

Let us look at the linear part of Eq. (A-3),

$$X''(x)-\frac{v}{D}\,X'(x)-K^2X(x)=0.$$

This equation is one of the standard forms for a linear differential equation. The solution is as follows:

$$m^2-\frac{v}{D}\,m-K^2=0,$$

$$m=\frac{\frac{v}{D}\pm\sqrt{\frac{v^2}{D^2}+4K^2}}{2},\quad m_1=\frac{\frac{v}{D}+\sqrt{\frac{v^2}{D^2}+4K^2}}{2},\quad m_2=\frac{\frac{v}{D}-\sqrt{\frac{v^2}{D^2}+4K^2}}{2},$$

* The solution to this equation is sketched in Wise and Ablow;[19] we are presenting here an expanded version of the solution and applying it to our particular case.

$$X(x) = A_i \exp\left\{\frac{1}{2}\left[\frac{v}{D} + \frac{v^2}{D^2} + 4K^2\right]^{\frac{1}{2}}x\right\} + B_i \exp\left\{\frac{1}{2}\left[\frac{v}{D} - \frac{v^2}{D^2} + 4K^2\right]^{\frac{1}{2}}x\right\}. \quad (A\text{-}4)$$

The radial part of Eq. (A-3) is

$$r^2R''(r) + r\,R'(r) + K^2r^2\,R(r) = 0. \quad (A\text{-}5)$$

If we make the substitution $y = kr$, Eq. (A-5) becomes

$$y^2R''(y) + yR'(y) + y^2\,R(y) = 0, \quad (A\text{-}6)$$

which is Bessel's equation of order zero.

The solution for this equation is

$$R(y) = C_3\,J_o(y) + C_4\,Y_o(y), \quad (A\text{-}7)$$

where $J_o(y)$ is a function defined by an infinite series known as the Bessel function of the first kind of order zero, and $Y_o(y)$ is a function defined by another infinite series known as the Bessel function of the second kind of order zero. Now the solution for Eq. (A-1) must be finite for $r = 0$. Therefore, since $Y_o(y) \to \infty$ as $y \to 0$, $C_4 = 0$. Equation (A-7) is now

$$R(y) = C_3\,J_o(y). \quad (A\text{-}8)$$

Let us apply the boundary condition,

$$\frac{\partial n\,(r=R,x)}{\partial r} = -\,n\,\frac{(R,x)}{\delta R}. \quad (A\text{-}9)$$

Since this condition applies only to the radial part, we may write it as

$$R'(kr)\Big|_{r=R} = -\,\frac{R(kR)}{\delta R}.$$

Performing the indicated operations, we get

$$C_3\,k\,J_1(kR) = \frac{C_3}{\delta R}\,J_o(kR).$$

Let $k = \frac{a}{R}$, where a is a constant; then

$$J_o(a) = \delta\ a\ J_1(a). \tag{A-10}$$

The roots of Eq. (A-10) are α_i (i = 1,2,3,4,...), and have been tabulated by Wise and Ablow for various values of δ.

Now the solution to the radial part is

$$R(r) = \sum_{i=1}^{\infty} J_o\left(\frac{\alpha_i r}{R}\right), \qquad \text{where } k = \frac{\alpha_i}{R},$$

and the solution to the linear part is

$$X(x) = \sum_{i=1}^{\infty} (A_i\ e^{m_1 x} + B_i\ e^{m_2 x}).$$

Combining these two equations, we get

$$n(r,x) = \sum_{i=1}^{\infty} \left(A_i e^{\left\{\frac{1}{2}\left[\frac{v}{D} + \left(\frac{v^2}{D^2} + 4K^2\right)^{\frac{1}{2}}\right]x\right\}} + B_i e^{\left\{\frac{1}{2}\left[\frac{v}{D} - \left(\frac{v^2}{D^2} + 4K^2\right)^{\frac{1}{2}}\right]x\right\}}\right.$$

$$\left. x\ J_o\left(\frac{\alpha_i r}{R}\right)\right). \tag{A-11}$$

At x = 0, n = n_o, therefore

$$n_o = \sum_{i=1}^{\infty} (A_i + B_i)\ J_o\left(\frac{\alpha_i r}{R}\right). \tag{A-12}$$

At x = ∞, n = 0, so A_i = 0 for this boundary condition to be true.

Therefore

$$n_o = \sum_{i=1}^{\infty} B_i\ J_o\left(\alpha_i \frac{r}{R}\right). \tag{A-13}$$

If we multiply both sides of Eq. (A-13) by $\left(\frac{r}{R}\right) J_o\left(\frac{\alpha_k r}{R}\right)$ and use the orthogonal properties of Bessel functions, we obtain,

$$\int_0^R \left(\frac{r}{R}\right) J_o\left(\frac{\alpha_i r}{R}\right) J_o\left(\frac{\alpha_k r}{R}\right) d\left(\frac{r}{R}\right) = \begin{cases} 0 & \text{for } i \neq k \\ \frac{1}{2}\left(1+\delta^2\alpha_i^2\right) J_1^2(\alpha_i) & \text{for } i = k \end{cases}$$

and also

$$\int_0^R \left(\frac{r}{R}\right) J_o\left(\frac{\alpha_i r}{R}\right) d\left(\frac{r}{R}\right) = \frac{J_1 \alpha_i}{\alpha_i},$$

we find

$$B_i = \frac{2n_o}{\alpha_i}\left[\left(\alpha_i^2\delta^2+1\right) J_1(\alpha_i)\right]^{-1},$$

$$\frac{n}{n_o} = 2\sum_{i=1}^{\infty} \frac{\exp\left\{\frac{1}{2}\left(\frac{v}{D} - \left[\frac{v^2}{D^2} + \left(2\frac{\alpha_i}{R}\right)^2\right]^{\frac{1}{2}}\right) x\right\}}{\alpha_i\left(\alpha_i^2\delta^2 + 1\right) J_1(\alpha_i)} J_o\left(\frac{\alpha_i r}{R}\right). \quad \text{(A-14)}$$

For the conditions that interest us, we have $\delta \geq 10^3$ ($\gamma \approx 10^{-5}$), and by use of the tables in Wise and Ablow, it can be shown that only the first term in the series in Eq. (A-14) is important.

Then $J_o\left(\frac{\alpha_i r}{R}\right) \approx 1$, $0 \leq r \leq R$, $\alpha_i \approx \left(\frac{2}{\delta}\right)^{\frac{1}{2}}$, and $J_1(\alpha_i) \approx \frac{\alpha_i}{2}$. If we make these substitutions into Eq. (A-14) and also $\delta = \frac{4D}{\gamma c R}$, we obtain Eq. (10) in Part III,

$$\frac{n}{n_o} = \exp\left[\frac{1}{2}\left(\frac{v}{D} - \left[\frac{v^2}{D^2} + \frac{2\gamma c}{DR}\right]^{\frac{1}{2}}\right) x\right].$$

We shall now solve the differential equation (A-1) with an additional term linear in n. The equation is

$$D\left[\frac{1}{r}\frac{\partial}{\partial r}\left(r\frac{\partial n}{\partial r}\right) + \frac{\partial^2 n}{\partial x^2}\right] - v\frac{\partial n}{\partial x} - k_1 n = 0. \quad \text{(A-15)}$$

Separating variables as we did previously, we find

$$\frac{R''(r)}{R(r)} + \frac{1}{r}\frac{R'(r)}{R(r)} = \frac{-X''(x)}{X(x)} + \frac{v}{D}\frac{X'(x)}{X(x)} + \frac{K_1}{D} = -K^2 \qquad \text{(A-16)}$$

We see from Eq. (A-16) that the radial part is the same as previously. The same boundary conditions also apply to this problem. Now let $Z = \frac{K_1}{D} + K^2$.

Then the linear part is

$$X''(r) - \frac{v}{D} X'(x) - Z X(x) = 0.$$

This equation is similar to the linear equation solved previously. By analogy to that solution we get

$$\frac{n}{n_o} = 2 \sum_{i=1}^{\infty} \frac{\exp\left\{\frac{1}{2}\left[\frac{v}{D} - \left(\frac{v^2}{D^2} + 4G\right)^{\frac{1}{2}}\right] x\right\}}{\alpha_i (1 + \delta^2 \alpha_i^2) J_1(\alpha_i)} . \qquad \text{(A-17)}$$

The same approximations hold for this problem, and by substituting into Eq. (A-17) we can derive Eq. (13) in Section III,

$$\frac{n}{n_o} = \exp\left[\frac{1}{2}\left(\frac{v}{D} - \left[\frac{v^2}{D^2} + \frac{4k_1}{D} + \frac{2\gamma c}{DR}\right]^{\frac{1}{2}}\right)x\right].$$

BIBLIOGRAPHY

1. Sanders, Schawlow, Dousmanis, and Townes, Phys. Rev. 53, 1158 (1953).
2. E. B. Brackett, The Use of Dielectric Rod Waveguides for the Microwave Spectra of Free Radicals, (Ph.D. Thesis), University of California, Berkeley, 1957.
3. R. T. Meyer, Free Radical Microwave Spectroscopy, (Ph.D. Thesis), University of California, Berkeley, 1961.
4. R. Beringer and M. A. Heald, Phys. Rev. 95, 1474 (1954).
5. T. M. Shaw, J. Chem. Phys. 30, 1366 (1959).
6. T. M. Shaw, J. Chem. Phys. 31, 1142 (1959).
7. Hildebrandt, Booth, and Barth, J. Chem. Phys. 31, 273 (1959).
8. Hildebrandt, Barth, and Booth, Planetary and Space Sci. 3, 194 (1961).
9. H. E. Radford, Phys. Rev. 122, 114 (1961).
10. M. Tinkham and M. W. P. Strandberg, Phys. Rev. 97, 937 (1955).
11. S. N. Foner and R. L. Hudson, J. Chem. Phys. 23, 1364 (1955).
12. A. J. B. Robertson, Discussions Faraday Soc. 17, 98 (1954).
13. R. H. Burgess and J. C. Robb, in Reactions of Free Radicals in the Gas Phase, Special Publication No. 9, (Chemical Society, London, 1957), p. 167.
14. O. Oldenberg and E. F. Riecke, J. Chem. Phys. 7, 485 (1939).
15. W. V. Smith, J. Chem. Phys. 11, 110 (1943).
16. H. G. Poole, Proc. Roy. Soc. (London) 163, 404 (1937).
17. W. Steiner, Trans. Faraday Soc. 31, 623 (1935).
18. W. Steiner, Trans. Faraday Soc. 31, 962 (1935).
19. H. Wise and C. M. Ablow, J. Chem. Phys. 29, 634 (1958).

20. K. J. Laidler, J. Phys. Chem. 53, 712 (1949).

21. H. Wise and C. M. Ablow, J. Chem. Phys. 35, 10 (1961).

22. S. Krongelb and M. W. P. Strandberg, J. Chem. Phys. 31, 1196 (1959).

23. L. M. Beebe, Mixed Train Daily, a Book of Short-Line Railroads, (E. P. Dutton, New York, 1947).

24. J. C. Greaves and J. W. Linnett, Trans. Faraday Soc. 55, 1338 (1959).

25. J. P. Wittke and R. H. Dicke, Phys. Rev. 103, 620 (1956).

26. J. Crank, The Mathematics of Diffusion, (Oxford University Press, London, 1956).

27. A. Fick, Ann. Physik, 170, 59 (1855).

28. H. Motz and H. Wise, J. Chem. Phys. 32, 1893 (1960).

29. I. Amdur, J. Chem. Phys. 4, 339 (1936).

30. R. L. Collins and J. W. Hutchins, Bull. Am. Phys. Soc. 7, 114 (1962).

31. H. Wise, J. Chem. Phys. 31, 1414 (1959).

32. N. N. Semenoff, Acta Physicochim. U.R.S.S. 18, 93 (1943).

33. V. Bursian and V. Sorokin, Z. physik. Chem. B 12, 247 (1931).

34. R. R. Baldwin, Trans. Faraday Soc. 52, 1337 (1956).

35. Hirschfelder, Curtiss, and Bird, Molecular Theory of Gases and Liquids (John Wiley and Sons, Inc., New York, 1954), p. 579.

36. C. R. Wilke, Chem. Eng. Progr. 46, 95 (1950).

37. Bruce Mahan, (University of California), private communication.